



HAL
open science

Applying Full-Field Measurement Techniques for the Thermomechanical Characterization of Shape Memory Alloys: A Review and Classification

D. Delpueyo, A. Jury, Xavier Balandraud, M. Grédiac

► **To cite this version:**

D. Delpueyo, A. Jury, Xavier Balandraud, M. Grédiac. Applying Full-Field Measurement Techniques for the Thermomechanical Characterization of Shape Memory Alloys: A Review and Classification. *Shape Memory and Superelasticity*, 2021, 7 (4), pp.462-490. 10.1007/s40830-021-00355-w . hal-04004968

HAL Id: hal-04004968

<https://hal.science/hal-04004968>

Submitted on 25 Feb 2023

HAL is a multi-disciplinary open access archive for the deposit and dissemination of scientific research documents, whether they are published or not. The documents may come from teaching and research institutions in France or abroad, or from public or private research centers.

L'archive ouverte pluridisciplinaire **HAL**, est destinée au dépôt et à la diffusion de documents scientifiques de niveau recherche, publiés ou non, émanant des établissements d'enseignement et de recherche français ou étrangers, des laboratoires publics ou privés.

Applying full-field measurement techniques for the thermomechanical characterization of Shape Memory Alloys: a review and classification

D. Delpueyo A. Jury X. Balandraud[†] M. Grédiac

Université Clermont Auvergne
CNRS, SIGMA Clermont, Institut Pascal
F-63000 Clermont-Ferrand, France

[†]Corresponding author, xavier.balandraud@sigma-clermont.fr

Abstract

Full-field measurement techniques are now mature. As such, they have profoundly impacted the experimental mechanics community in recent years. The way shape memory alloys (SMAs) are now tested is not spare from this deep-rooted trend, as reflected by the increasing number of papers published in the SMA literature. In this context, the aim of this contribution is to give an overview of the use of full-field measuring techniques for SMA characterization purposes. We recall first the basic principle of one volume and four surface techniques employed in this community. Several typical papers where such techniques are employed are then presented, by highlighting in each case the extent to which the thermomechanical response of SMAs could be better understood and modeled thanks to these techniques. A classification by several criteria of about 300 references is finally offered and discussed. The main criteria are the type of SMA, the type of technique employed to perform the measurements, and the type of test.

Keywords Digital image correlation, Grid method, Infrared thermography, Mechanical behavior, Moiré interferometry, SMA, Thermomechanical characterization

1 General introduction

Performing thermomechanical tests on small-sized specimens is a core activity in mechanics of materials. Indeed, these tests enable the experimentalist to study the response of engineering materials, to observe various phenomena occurring while loading is in progress, to propose suitable constitutive laws modeling the response, and to identify the parameters governing these laws. This is all the more

important for Shape Memory Alloys (SMAs) because such materials feature peculiar properties such as superelasticity, damping or memory effect, which distinguish them from other metallic materials.

When testing materials, the classic route is to assume that the stress distribution is known a priori by using some simplifying assumptions and to measure the strain, the relationship between these two quantities providing the experimental stress-strain curve. For instance, with the most popular test, namely the tensile test, this stress distribution is assumed to be uniform and merely equal to the force divided by the cross-section of the specimen. The strain is then measured at some points of the surface of the specimen with strain gages, or on average over a region with an extensometer. The stress-strain curves which are deduced are obviously of significant interest for SMAs since they enable the user to compare the response of different alloys and to observe and quantify specific features such as stress plateaus or hysteresis loops. These curves are however not sufficient to clearly understand the physical phenomena which directly cause these features, such as the appearance and growth of new phases or microstructures. The reason is that these phenomena are generally localized and spatially distributed, so classic measurement means such as strain gages or extensometers cannot really reveal them. This limitation has caused the recent lure of full-field measurement techniques in the SMA community, as illustrated by the increasing use of such techniques to characterize these materials (in fact, this is a general trend which concerns all engineering materials [1]). The benefit of using these tools for SMA characterization is that they provide, within certain limits, the amplitude and localization of strain or temperature heterogeneities which are the consequence of the physical phenomena of interest.

In this context, the objective of this paper is to give a comprehensive overview of the literature on SMAs where full-field measurement techniques are employed for thermomechanical characterization purposes. We first start by briefly describing the different techniques which are available to obtain these measurements, and specify their main metrological performance. Then we focus on nine typical papers from the SMA literature where full-field measurement techniques are used, and highlight the findings which could be made thanks to the use of such measuring techniques. A classification of the papers where full-field surface measurement techniques are used to characterize SMAs is finally offered. Different criteria are used such as the type of alloy under test, the nature of the technique used or the type of test which is performed. We conclude by offering some suggestions for future studies in this research field.

2 Full-field methods used to characterize SMAs

Four surface and one 3D full-field measuring techniques have been identified in the papers of the literature dealing with SMA characterization. Concerning surface measurements, three of these four techniques, namely Digital Image Correlation (DIC), the Grid Method (GM) and Moiré Interferometry

(MI), are dedicated to displacement and strain field measurement. Infrared Thermography (IRT) concerns thermal measurements, infrared cameras directly providing temperature fields after thorough calibration. The volume measurement technique is 3D X-ray diffraction (3D-XRD), which aims at measuring 3D stress distributions. All these techniques are briefly presented in turn in the following sections.

2.1 Digital image correlation

DIC is a versatile full-field measurement technique, which is now wide-spread in the experimental mechanics community. It consists first in depositing a random pattern onto the surface of the specimen under study in order to enhance the contrast in the corresponding images when the natural one is not sufficient. This is merely obtained by paint spraying these surfaces. The usual version of DIC consists then in considering small sub-images (called subsets) in the reference image, and in seeking their counterparts in the deformed one. This is made by iteratively minimizing, with respect to the sought displacement, the difference between the gray level distribution in deformed and reference subsets. This minimization finally provides the displacements at the center of the subsets. Strain fields are deduced by smoothing and spatially differentiating these quantities. More sophisticated approaches are also available, such as the global version of DIC. In this latter case, a priori knowledge on the displacement field is used in the formulation of the companion minimization problem, which is resolved in order to determine the parameters governing this model. Even a finite element model for the displacement field can be used. In this case, the displacement at the nodes are returned by DIC, the displacement in between being described by shape functions supposed to precisely model the displacement within the elements [2–4]. Images processed with DIC are taken with cameras equipped with CCD or CMOS sensors. One camera is enough for in-plane displacement measurement, while two cameras at least are necessary to perform stereo-DIC. **This version of DIC is used to estimate 3D-displacement fields on the specimen surface. The surfaces over which measurements are made with DIC are typically several cm² in size but this technique can also be used at the microscale with SEM [5–8]. DIC is sometimes coupled with EBSD to correlate the results with crystal orientations, as illustrated later on in this paper.**

It is difficult to summarize the metrological performance of DIC with some figures. The reason is that compared to other classic local measurement means such as strain gages, a new quantity appears here, namely the spatial resolution. This quantity is discussed in the literature (see Refs [4, 9–11] for instance) but it is not clearly defined in any standard, to the best of the authors' knowledge. In short, it reflects the ability of a measuring technique to reliably reveal close details in displacement or strain maps. The point is that this quantity changes as a function of some parameters arbitrarily set by the user such as the subset size. With commercially available DIC packages, it can be said that the strain

resolution can typically reach 10^{-3} over small zones having some millimeters in size, with a field of view equal to some squared centimeters [10, 11]. More detail on DIC can be found in Ref. [12] for instance.

2.2 The grid method

DIC is user-friendly but also has some disadvantages. First, random speckles do not constitute the optimal pattern with respect to sensor noise propagation [13]. This is potentially an issue when the information only barely emerges from the noise floor. In the same way, employing a random pattern induces a pattern-induced bias (PIB) [14], especially in case of high-frequency strain distribution [15]. This is potentially the case when some microstructures like martensite needles appear in an austenitic specimen. Finally, DIC relies on a minimization problem, which is resolved iteratively. Thus the computational cost may be significant if large images are considered, or if refined pixelwise calculations are needed, or if a large number of images are to be processed. This has led some authors to consider alternative approaches such as the Grid Method (GM), which consists in relying on periodic patterns instead of random ones. In this case, the periodic pattern is considered as a carrier and the displacement at any point as a modulation of the phase of this carrier. Fourier analysis is employed to extract this modulation and retrieve the displacement field from the images. The benefit is that the noise in final maps caused by sensor noise propagation is lower than with DIC [9], if not minimal when periodic patterns such as checkerboards are used [16]. In Ref. [17], it is shown that *ceteris paribus*, the compromise between spatial resolution and noise affecting displacement maps due to camera sensor noise propagation is about three times better with checkerboard images processed with a suitable spectral method than with speckle images processed with DIC. In addition, PIB is minimized (if not virtually eliminated) with periodic patterns [14, 16]. The strain maps deduced by differentiating displacement maps can even be enhanced by using deconvolution, all spatial frequencies involved in the strain maps being then provided without any bias up to a certain cutoff frequency [16]. Finally, the determination of the displacement is very fast, the calculation being performed in the Fourier domain [9, 16, 18]. Note that this technique can also be applied at microscale [19], but no use on SMA **at small scale** has been reported in the literature to the best of the authors' knowledge. A first limitation of the grid method is that only 2D measurements on flat specimens can be performed with the present version of this technique even though out-of-plane measurements are potentially measurable. The second one is that depositing periodic patterns onto flat surfaces requires more time and effort than depositing a speckle for DIC [20]. Indeed, speckle patterns can be deposited with a mere airbrush for instance. It means that the use of periodic patterns is justified only in situations for which a good compromise between spatial resolution and measurement resolution is required to reliably observe displacement and strain maps on flat specimens, and/or if many images are to be

processed, which is potentially the case with SMAs.

2.3 Moiré interferometry

Moiré interferometry (MI) extends the range of conventional moiré to measure displacements with very high sensitivity. A diffraction grating is first deposited onto the surface of the specimen. Its frequency typically lies between some hundreds to some thousands of lines per millimeter, depending on the desired resolution for the measuring system. This grating is then illuminated by two beams of coherent light, which are inclined with respect to the normal of the surface of the specimen. The angle of one beam is the opposite of the other, so these beams generate interferences in the zone of their intersection. The resulting virtual grating acts as the reference grating of classic moiré arrangement, the deformed grating being the one deposited onto the surface of the specimen. Both gratings interact and thus form moiré fringes, which are captured by a camera. The fringe images recorded during a test are then processed like those of classic moiré to deduce the displacement field. Among the three methods presented here (DIC, GM and MI), the latter is certainly the one which provides the highest sensitivity. For instance, Ref. [21] reports that with a diffraction grating of 1,300 lines per millimeter and a wavelength of 500 nm for the light, two consecutive fringes represent a difference of 350 nm for the displacement. It should therefore be employed in situations for which the displacement remains of low amplitude. Otherwise, the number of fringes may become too large to be processed to extract the sought displacement field. More details on this technique are available in Refs [22–25] for instance.

2.4 Infrared thermography (IRT)

Infrared (IR) thermography enables temperature measurement without any contact, directly from the electromagnetic waves emitted by an object in suitable ranges of wavelengths, namely between 1.7 μm and 14 μm [26]. There are two types of IR detectors: photon detectors and thermal detectors. In general, photon detectors have better performance with reduced integration time, better sensitivity, and reduced noise compared to thermal detectors. Such detectors must however be cooled to a temperature close to that of liquid nitrogen, thus requiring a sterling engine embedded in the camera. "Cooled" cameras are often used for research in thermomechanics of materials. Specific precautions must be taken for quantitative measurements. Some metrological considerations must also be taken into account [27]. As each IR detector of the focal plane array has its own response, a Non-Uniformity Correction procedure must be performed using a black body. The thermal emissivity of the surface of the material sample under study must also be known. For metals, it is advisable to use high emissivity paints, which are applied onto the specimen surface, but paint adherence issues may occur when the specimen deforms. When the surface of the specimen is curved (*e.g.* for wires or cylinders), the apparent emissivity changes as a function of the angle of view of the camera. However, it remains relatively

constant up to a certain angle, which allows a simple processing of the raw output of the camera for a temperature measurement along a generatrix of a wire for example. Even for a thermal emissivity close to one, the temperature of the specimen environment must also be known to subtract remaining reflections. More generally, parasitic reflections must be minimized. A dummy specimen placed next to the mechanically tested one can be used for this purpose. An IR thermographic system is characterized by its so-called Noise Equivalent Temperature Difference (NETD) and by the spatial resolution of the thermal images. NETD corresponds to one standard deviation of the measurement noise, namely the temperature resolution. Cooled cameras can reach a NETD of about 20 mK in optimized conditions, with more than one million pixels for the latest generation of cameras.

In the context of thermomechanical characterization of materials, the analysis of temperature fields is difficult because of heat diffusion within the specimen. A heat exchange also takes place between specimen and its environment, for instance with the jaws of the testing machine and the ambient air. However, IR thermography can be employed to assess the fields of heat power density (simply called "heat source") produced or absorbed by the material due to a change in its mechanical or crystalline state. The reconstruction of heat sources can be performed using suitable versions of the heat diffusion equation. Two main approaches are available in the literature to estimate heat sources in thermomechanics of materials: by minimizing the error between measured temperature fields and theoretical temperature fields provided by a model [28]; or by directly calculating the terms of the heat equation from experimental thermal data [29]. A critical point in the latter approach is the estimation of the conduction term. Indeed, this term involves second partial derivatives and these quantities are strongly impacted by noise which unavoidably affects thermal images.

2.5 3D X-ray diffraction

3D X-ray diffraction (3D-XRD) has emerged in the last 20 years [30, 31]. This is a microscopy technique for volume measurement performed by using X-ray energy between 30 and 100 keV. It enables the user to obtain the shapes and the crystal orientation of grains in polycrystalline specimens. For full-field measurements under mechanical loading, the strain tensor is measured on a grain-by-grain basis. **The technique also enables the experimentalist to reconstruct strain and stress distributions within individual grains by using small beams and large grains [32–34].** The stress tensor can then be deduced assuming a linear elastic behavior of the crystal. 3D grain maps of deformed polycrystalline specimens are reconstructed from individual diffraction spots. Each diffraction spot is obtained from the diffraction pattern, which gives the crystallographic parameters of the material. The strain tensor of each grain is obtained from the comparison between the undeformed and deformed configurations of the lattice. In polycrystalline materials, the resolution can be as low as about 1 μm in position and, after [35], the measurement resolution is 1E-04 for strain and 20 MPa for stress.

The main advantage of 3D-XRD is that no specimen preparation is required. In addition, large and complex shaped specimens can be studied. **The rate of the data acquisition depends on the size of the beam and the region of interest, the instrumentation, and the speed of the detector. The acquisition can be fast enough to allow measurements in a few minutes.** Full details on this technique can be found in Ref. [30].

3 Focus on some typical examples of SMA characterization with full-field surface measurement techniques

There are many papers available in the literature, which report studies where full-field surface measurement techniques are used to characterize SMAs. A classification will be given later on in this paper. Providing a short review of all of them is out of the scope of the present contribution. It is however of interest to focus on a limited number of references, which typically reflect the benefit of using full-field measurement techniques for SMA characterization. Hence the aim of this section is to briefly present some of these papers, by highlighting in each case the type of SMA which was studied, the type of specimen, test and measuring technique which were employed, as well as the phenomena that could be observed and analyzed mainly thanks to the fact that full-field measurement techniques were employed instead of classic measuring tools.

3.1 Example 1: performing DIC and IRT on NiTi wires [36]

NiTi SMAs are mainly commercially available as wires, so many studies report results obtained with tensile tests performed on wire specimens. Ref. [36] provides various tips and tricks for the best characterization of such specimens with DIC and IRT. The authors present strain and temperature distributions during the mechanical stabilization of a superelastic wire over several cycles. Indeed, a repeatable behavior is crucial for successfully employing SMAs in engineering applications. Since as-received straight annealed NiTi wires are known to exhibit significant changes in their response during the first transformation cycles (mechanical training), the authors observed the evolution of the strain and temperature fields during the first load-unload cycles at constant macroscopic strain rate. In addition to discussing the experimental results, the authors give practical recommendations concerning specimen preparation, experimental setup and data post-processing. Stereo-DIC was applied to measure the longitudinal strain. Figures 1-a and -b show typical strain and temperature maps, respectively. They were obtained at the same time, during the loading phase of a superelastic NiTi wire. It can be seen in Figure 1-b that the strain distribution enables us to precisely locate a transformation front between austenite (A) and martensite (M^+) thanks to the sudden strain increase. The 1D distribution of the longitudinal strain was then plotted over time during the first cycles of the test, which

gives Figure 1-c. The spatiotemporal kinetics of the transformation is evidenced in this figure thanks to the high difference between the strain level in austenite and martensite. Over the cycles, one or several transformation fronts are thus tracked in parallel to the evolution of the engineering stress, see the black curves superposed to the spatiotemporal strain distribution in Figure 1-c. The authors also show that it is possible to distinguish the actual material response and possible experimental problems such as slippage of the specimen in the jaws of the testing machine. This phenomenon sometimes appears with SMA wires, when phase transformation occur in the clamped zones.

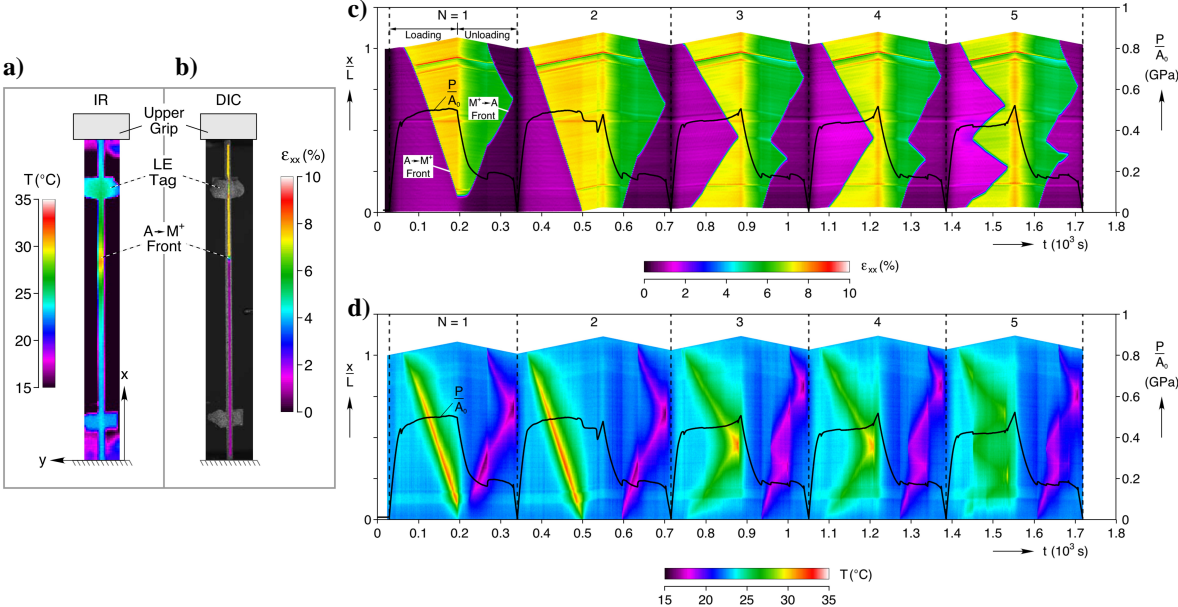


Figure 1: Analyzing with DIC and IRT the mechanical stabilization of a superelastic NiTi SMA wire, after [36].

As $A \rightarrow M^+$ and $M^+ \rightarrow A$ transformations are accompanied by latent heat release and absorption, coupling strain and temperature measurements provides additional information where the spatiotemporal distribution of the temperature along the specimen is shown, see Figure 1-d. In their paper, the authors discuss the changes observed in Figures 1-c and -d as well as their coupling. It can be seen that deducing the location of the transformation fronts from the temperature distribution is more difficult because of heat diffusion within the specimen (see next section). **Heat diffusion tends to smooth out the temperature fields over time.** Thus, by nature, the temperature change distribution is often smoother than the strain distribution. However, this paper illustrates the fact that the spatiotemporal thermal signature is complementary to the mechanical response.

3.2 Example 2: performing deformation calorimetry in a superelastic NiTi SMA wire by IRT and heat source reconstruction [37]

As temperatures are impacted by heat diffusion within the specimen and heat exchange with the environment, another option for the analysis of thermal maps is to retrieve the heat source distribution from the temperature distribution by using the heat diffusion equation. It is worth remembering that a heat source is defined here as the power density of heat produced or absorbed by the material itself (in $\text{W}\cdot\text{m}^{-3}$ or in $\text{K}\cdot\text{s}^{-1}$ when multiplied by the volumetric heat capacity as in Figure 2). Ref. [37] is a typical example of this type of deformation calorimetry. In this study, the authors performed a superelastic cycle on a wire specimen made of stabilized NiTi SMA. The response of this specimen was studied with IR thermography. In addition to considering the heat source distribution instead of the temperature distribution, a difference with the preceding example is that the test is performed here at constant force rate instead of constant displacement rate. A consequence is that the plateau of the stress/strain curve is crossed at a much higher rate, enforcing the specimen to transform quickly. Figure 2-a shows the spatiotemporal distribution of the temperature change in this specimen during the test. Rapid increase and decrease in temperature logically follow the rapid changes in engineering strain (black curve): see the four thermal waves in Figures 2-b and -c respectively (two waves upon loading and two waves upon unloading). The main point here is that the spatiotemporal transformation kinetics is much better revealed by considering the heat source distribution depicted in Figures 2-d and -e than the temperature change distribution depicted in Figures 2-b and -c. Associating these heat sources with thermomechanical couplings enabled then the authors to identify martensite nucleation events (1 to 10) and martensite merging events (11 to 20) upon loading, as well as austenite nucleation events (21 to 30) and austenite merging events (31 to 41) upon unloading. Based on the heat source data, the authors found that the mechanical dissipation heat associated with the nucleation and melting events corresponds to about 25% of the released/absorbed latent heat.

3.3 Example 3: examining with stereo-DIC the response of a NiTi tube subjected to tensile, compression and bending tests [38]

Although NiTi SMAs are mainly available in the form of a wire, other shapes such as tubes can also be found. Consequently, other tests than the classic tensile test such as compression or bending can be performed in this case, and full-field measurements reveal other phenomena. In this spirit, stereo-DIC was used in Ref. [38] to obtain the axial strain fields on the outer surface of a superelastic NiTi tube. Uniaxial compression and four-point bending were applied on a tube specimen in addition to uniaxial tension. Figure 3 shows typical strain maps obtained during these tests. In tension, propagation fronts are classically observed upon loading (maps 2 to 7 in Figure 3-a) and unloading (8 to 12). Finger-shaped strain patterns inclined with respect to the loading direction are clearly visible at the interface

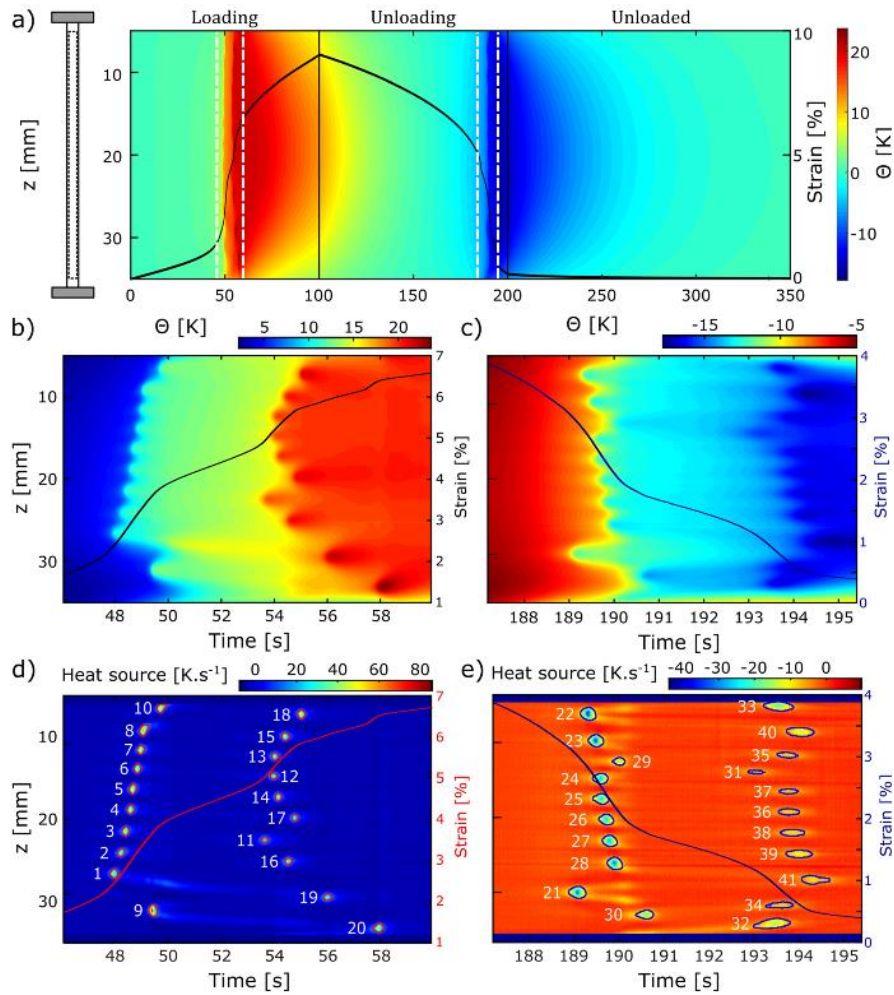


Figure 2: Analyzing with IRT and heat source reconstruction the calorific response of a stabilized NiTi SMA wire subjected to a force-controlled superelastic cycle, after [37].

between the austenite and martensite zones. In compression, no such localization was observed, neither upon loading (maps 2 to 7 in Figure 3-b) nor upon unloading (8 to 12), although a transient buckling was evidenced in map 10. Consistently with the tension-compression asymmetry, the bending test revealed strain localization in the part of the specimen subjected to tension, and no localization in the other part subjected to compression. A shift of the neutral axis toward the compression side can also be observed, see Figure 3-c. DIC strain measurements provide details enabling the authors to discuss the classic assumptions of elementary beam theory in the case of SMAs.

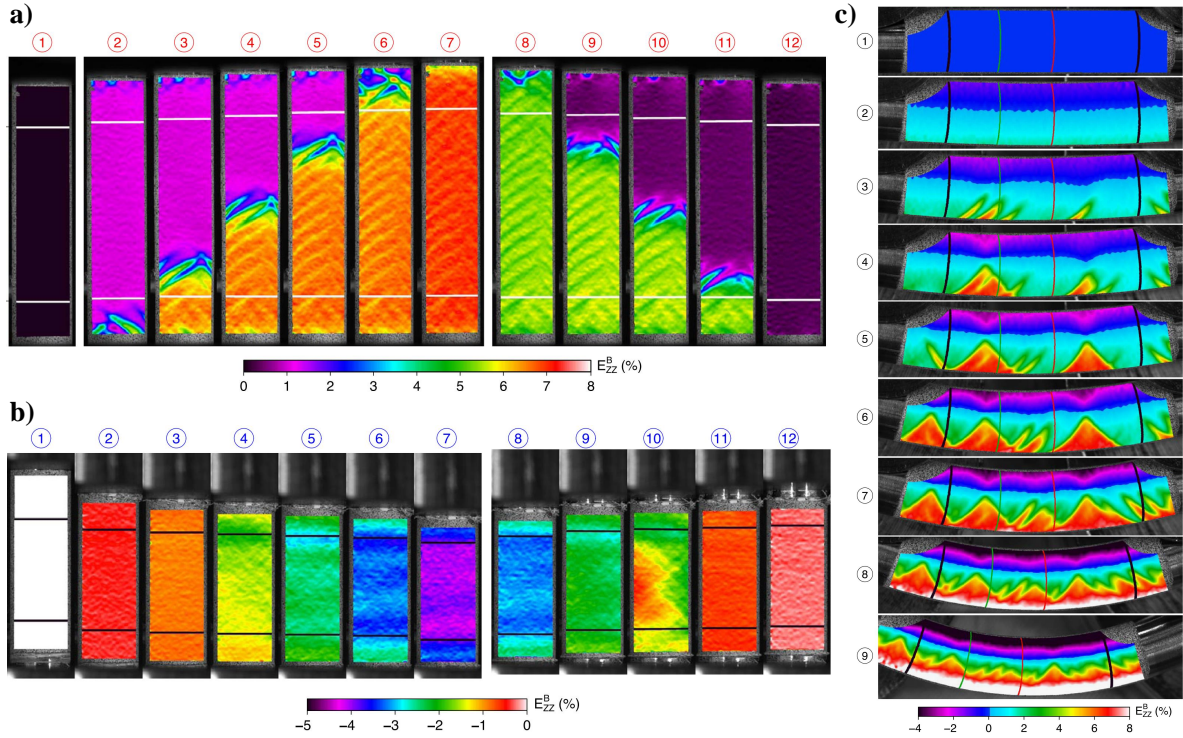


Figure 3: Analyzing with stereo-DIC the strain distribution at the outer surface of a superelastic NiTi tube subjected to: a) uniaxial tension, b) uniaxial compression and c) four-point bending, after [38].

3.4 Example 4: comparing at different temperatures the strain fields measured with DIC in a superelastic NiTi thin sheet [39]

In experimental mechanics, DIC is mainly used to observe 2D displacement and strain fields on the outer surface of flat specimens, so there are many such examples in the SMA literature. Ref. [39] discusses for instance the transformation kinetics in a flat superelastic NiTi thin specimen. The authors mainly focus on the difference in the mechanical response observed for different ambient temperatures. In particular, the stress plateau upon unloading tends to disappear and the residual strain to increase as the temperature increases. Figure 4 shows 2D maps of the longitudinal strain in uniaxial tension. They were obtained at 25°C and 100°C. Strain localization is observed upon loading at 25°C and 100°C. The sharp transitions between low-strain and high-strain regions can be observed in Figures 4-a and -b. They correspond to austenite and martensite, respectively. The same phenomenon occurs upon unloading at 25°C, whereas the reverse phase transformation appears to be homogeneous at 100°C. Coupling DIC measurements obtained during a set of various experiments with a suitable model enabled the authors to discuss the impact of local strain rate on the residual strain obtained at the end of the unloading stage.

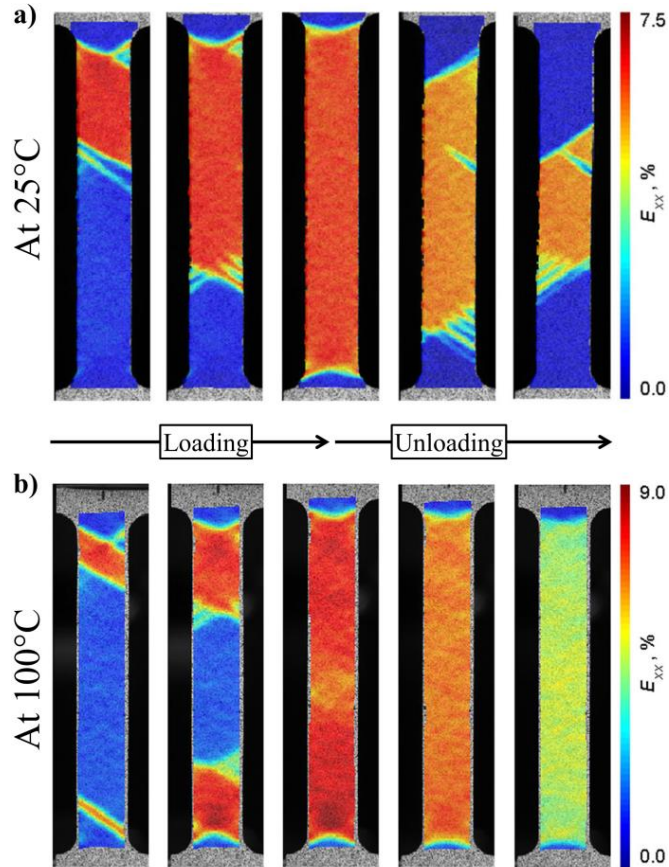


Figure 4: Comparing with DIC the strain fields in a superelastic NiTi thin sheet at two ambient temperatures, after [39].

3.5 Example 5: revealing with GM the microstructures appearing in a superelastic CuAlBe flat single-crystal [40]

As mentioned in Section 2 above, DIC is the most popular full-field measurement technique but it suffers from some limitations. In particular, recent papers [9, 17] clearly show that using regular patterns instead of random ones and processing the corresponding images with a spectral technique instead of DIC lead to displacement and strain maps with a better compromise between spatial resolution and measurement resolution. This favors the observation of localized phenomena like those occurring during phase transformation in SMA specimens. This is the reason why GM has been used in Ref. [40] to study the microstructures which appear in a superelastic CuAlBe flat single-crystal subjected to a tensile test. Figure 5 shows typical longitudinal strain maps obtained at different stages of the test. Martensite needles, habit planes and martensite twins were identified, see also the video attached to the online version of Ref. [40]. Despite the absence of macroscopic residual strain at the end of the mechanical cycle observed in Figure 5-a, significant differences were observed in terms of microstructures between

the loading and unloading phases. While loading was simply accompanied by the nucleation and merging of parallel martensite needles, see Figure 5-b, a much more complex microstructure evolution is revealed upon unloading in Figure 5-c, which may explain a part of the mechanical hysteresis.

With full-field measurement techniques, experimentalists have easy access to other strain components than the longitudinal one during uniaxial mechanical loading, which gives valuable information to analyze phenomena occurring in the specimen under test. For instance, the transverse strain map depicted in Figure 5-d shows that a different martensite variant is involved at the bottom part of the specimen. It is separated from the already transformed zone by a thin austenite band, which accommodates the two martensite variants and thus prevents the specimen from full transformation to martensite.

3.6 Example 6: applying DIC to reveal microstructures at the grain scale [41]

While single- and multi-crystals can be used to have large martensitic microstructures in copper-based SMAs, a need for measurements at microscale is required in order to better understand the thermomechanical response of NiTi. Small-scale full-field measurement techniques can again help the experimentalist get valuable information to reach this goal. As an example of such measurements, Figure 6 shows longitudinal strain fields extracted from SEM images and high-definition DIC applied on several grains with a mean size of $35\ \mu\text{m}$ [41]. Strain fields for the maximum value of the uniaxial loading (Figure 6-a) and after unloading (Figure 6-c) show that a part of the strain was recovered (Figure 6-b). Interesting conclusions were drawn by the authors by correlating strain maps with EBSD maps. By analyzing the orientation of the interfaces and considering Schmid factors, the authors showed that recoverable strain is due to the martensitic transformation, for which more than one variant per grain can be activated. They also showed that the selection of martensite variant can be influenced by shear transmission across grain boundaries. The strain levels that were locally measured are in good agreement with their theoretical counterparts for single crystals. Besides, non-recoverable strains are shown to be due to deformation slip in austenite, twinning in martensite and residual martensite. The benefit of using a full-field measurement technique at small scale to explain phenomena observed at a greater scale, especially when coupled with other analysis means (here EBSD), is illustrated here since these conclusions could not be drawn from classic global stress-strain curves.

3.7 Example 7: characterizing sharp austenite/martensite interfaces with moiré interferometry [42]

A mention to the use of moiré interferometry (MI) can be made here concerning small-scale measurements. Since applications of this technique to SMAs are quite rare in the literature, comparison cannot be made here with other techniques in terms of quality of the obtained results. However, the potential

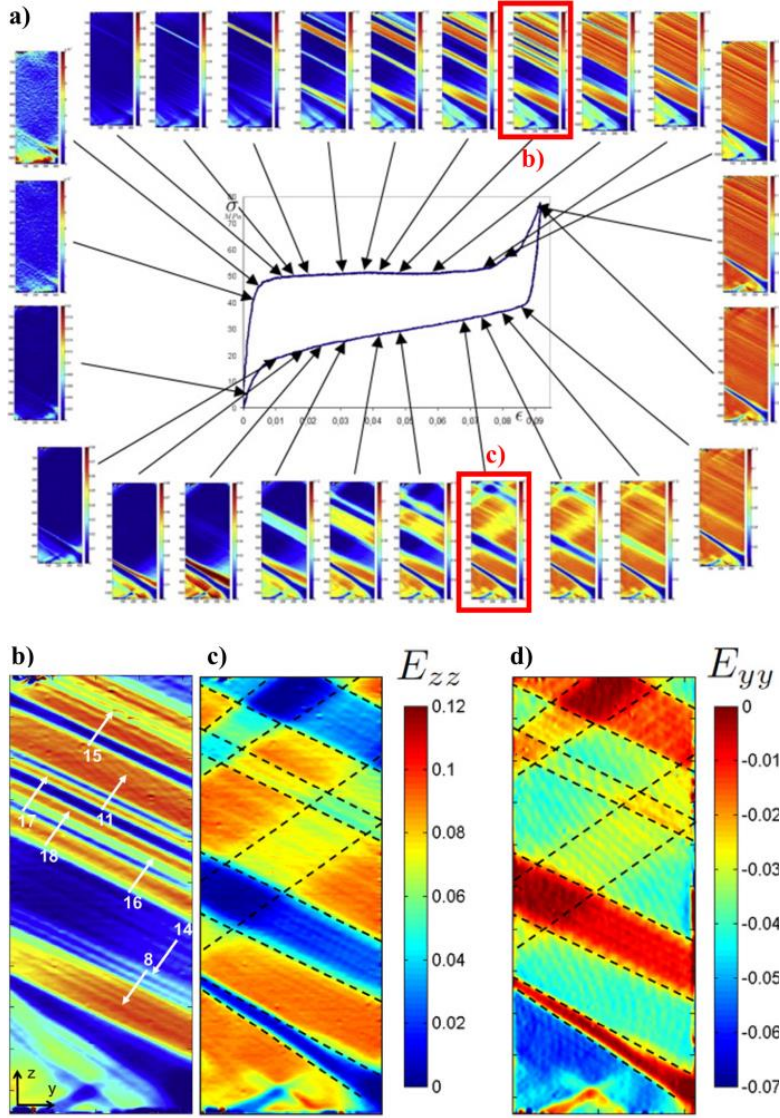


Figure 5: Employing GM to measure the strain distribution in a superelastic CuAlBe single-crystal, after [40] (see also the video available online).

of MI to provide information at the scale of the martensitic microstructures has been successfully demonstrated in some examples. For instance, Figure 7 shows the displacement fringe patterns in a shape-memory CuAlNi specimen after stress-induced transformation [42]. Several sharp interfaces between austenite and martensite are visible in a zone smaller than 1 mm^2 . Martensitic domains feature dense fringes (because of high strain level) compared to austenitic domains, where only elastic strains can be observed. Austenite wedges inside martensite are also evidenced. Various properties were extracted by the authors from the fringe distributions, such as the phase distribution, the strain jump over the interfaces and the orientation of the habit planes. Only moiré interferometry reveals

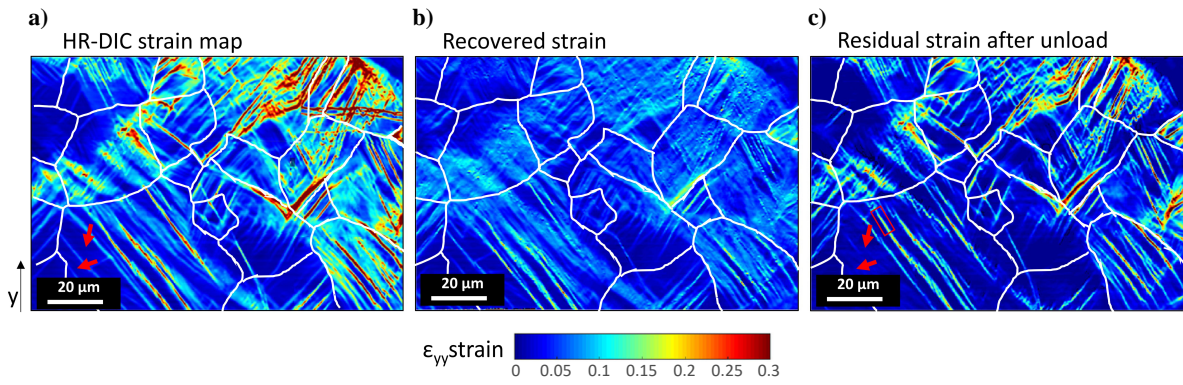


Figure 6: Studying at the grain scale with high-definition DIC a superelastic NiTi specimen subjected to uniaxial loading, after [41].

such sharp interfaces and allows such refined full-field measurements at the scale of microstructures.

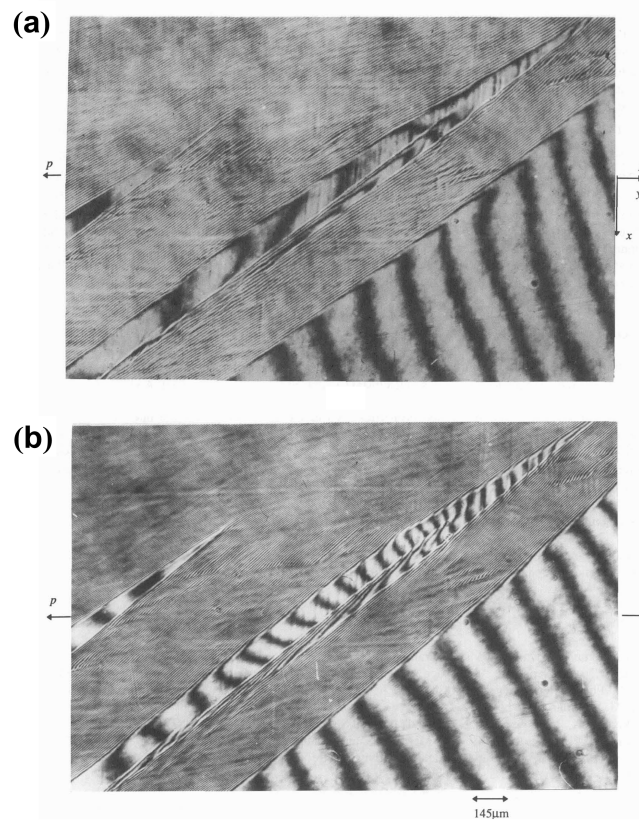


Figure 7: Employing moiré interferometry to observe microstructures in a shape-memory CuAlNi specimen after stress-induced transformation: a) horizontal displacement fringes, b) vertical displacement fringes, after [42].

3.8 Example 8: coupling DIC and IRT to perform deformation calorimetry [43]

A logical approach when studying SMAs is to couple full-field strain and temperature measurement techniques. The reason is that both the large strain levels (several percents) and the intense heat release/absorption (several kJ/kg) which are observed are the consequence of phase transformation. Ref. [43] is a typical example of such a coupling on a superelastic NiTi sheet subjected to a load-unload cycle in uniaxial tension. It also describes some practical aspects related to temporal and spatial synchronization. In particular, the authors discuss the difference in spatial resolution of the two systems used to obtain their measurements, namely DIC and IRT. Figures 8-a and -b show the variation in time of the 1D distribution of the longitudinal strain and the temperature change, respectively. Both distributions are displayed in the underformed/Lagrangian configuration. Indeed, the synchronization allowed temperature tracking at every material point during the deformation of the specimen. Heat sources could therefore be precisely reconstructed, see Figure 8-c. Finally, the temporal integration of the heat sources at every material points provided the value of the local heat produced along the test, see Figure 8-d. Beyond the precise analysis of the spatiotemporal transformation kinetics in NiTi SMAs, various technical aspects were studied in this paper such as the impact of the difference in thermal conductivity of austenite and martensite, which impacts heat source calculation. As a conclusion, such a coupled approach provides a truly comprehensive thermo-mechanical analysis once the practical implementation and processing difficulties are overcome.

3.9 Example 9: using 3D X-ray diffraction to reveal heterogeneous stress fields in a NiTi wire during a uniaxial tensile test [35]

The preceding examples deal with 2D measurements only. The reason is that except one paper which is discussed in this section, all the papers found in the literature concern surface measurements. As discussed in Section 2.5, X-ray diffraction allows strain tensor measurements in the bulk with the so-called 3D-X-ray technique. The stress tensor is then deduced grain by grain assuming that the constitutive equations are known a priori. To the best of the authors' knowledge, this technique has been applied only once for SMAs, namely in Ref. [35]. The objective was to observe the heterogeneity of the stress distribution in austenite in the vicinity of a martensitic band front (MBF), see Figure 9. The stress could not be evaluated in martensite because of the high number of refraction angles and the fact that the measurement resolution of the technique was not sufficient to detect all of them. Upstream of the MBF ($z > 125 \mu\text{m}$), a heterogeneity of the stress distribution is visible. Looking at the surface of the wire, the MBF classically appears to be large and perpendicular to the longitudinal axis. Thanks to 3D-XRD, it was possible to observe the shape of the MBF, which is a cone. The angle of this cone is about 55 deg, which is consistent with the results obtained in NiTi sheets and tubes

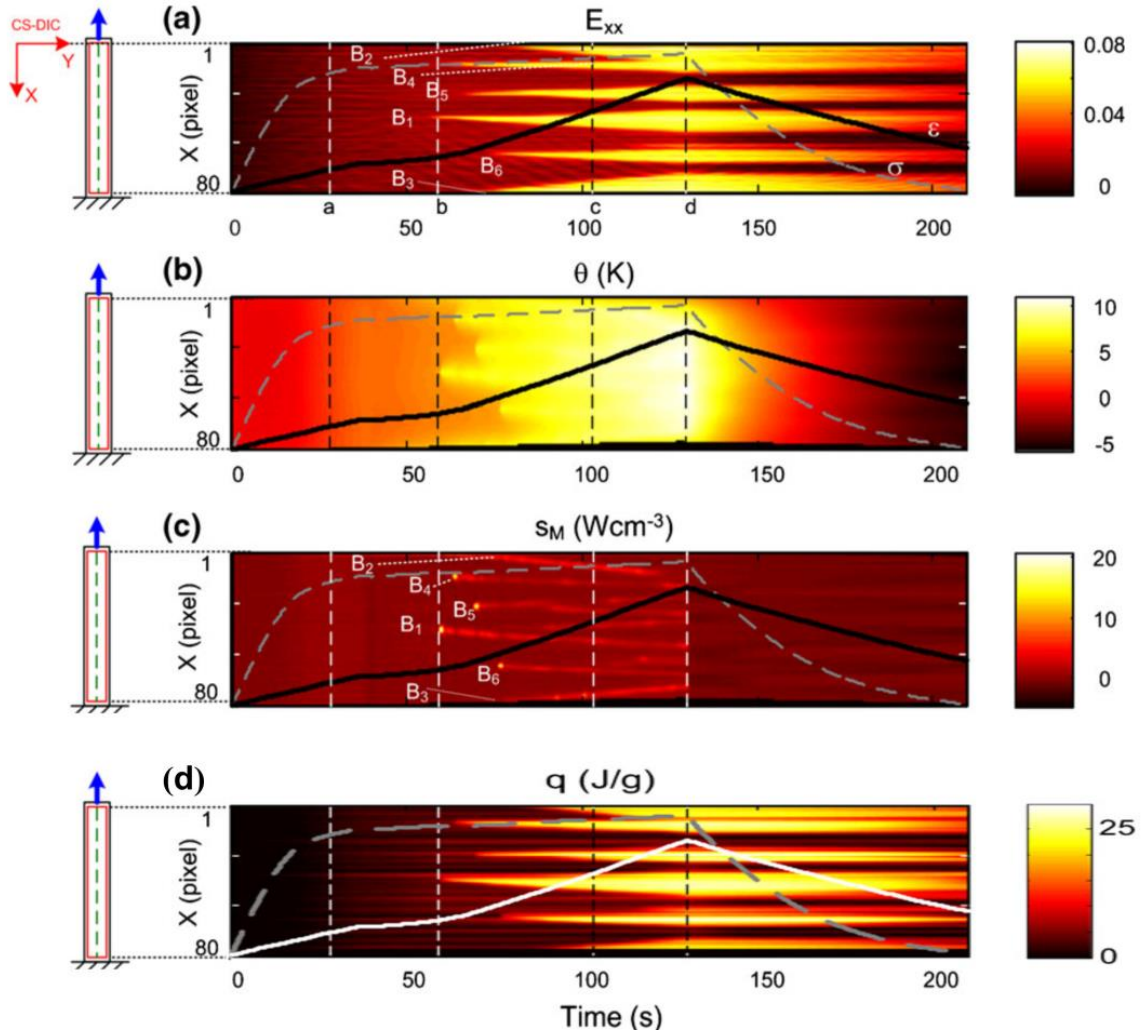


Figure 8: Coupling DIC and IR thermography for the thermomechanical analysis of a superelastic NiTi sheet specimen subjected to a uniaxial loading-unloading cycle: a) variation in time of the longitudinal strain distribution, b) same for the temperature changes, c) same for the heat sources, d) same for the heat, after [43].

with other techniques. This angle allows the minimization of the deformation incompatibilities at the macroscopic interface between the elastically deformed austenitic grains on the one hand (about 1%), and the grains already transformed into martensite on the other hand (about 10%). Beyond the axial stress component, the complete stress tensor was measured in the austenite grains to go further in the analysis. For example, it is shown that the principal direction attached to the maximum principal strain is aligned with the wire axis in all the grains except those located on the conical interface between austenite and martensite, see additional figures attached to Ref. [35]. The main results of the study are that the local stress in austenite grains is modified ahead of the nose of the cone-shaped

buried interface where the martensitic transformation begins, and that elevated shear stresses at the conical interface explain why the transformation is localized.

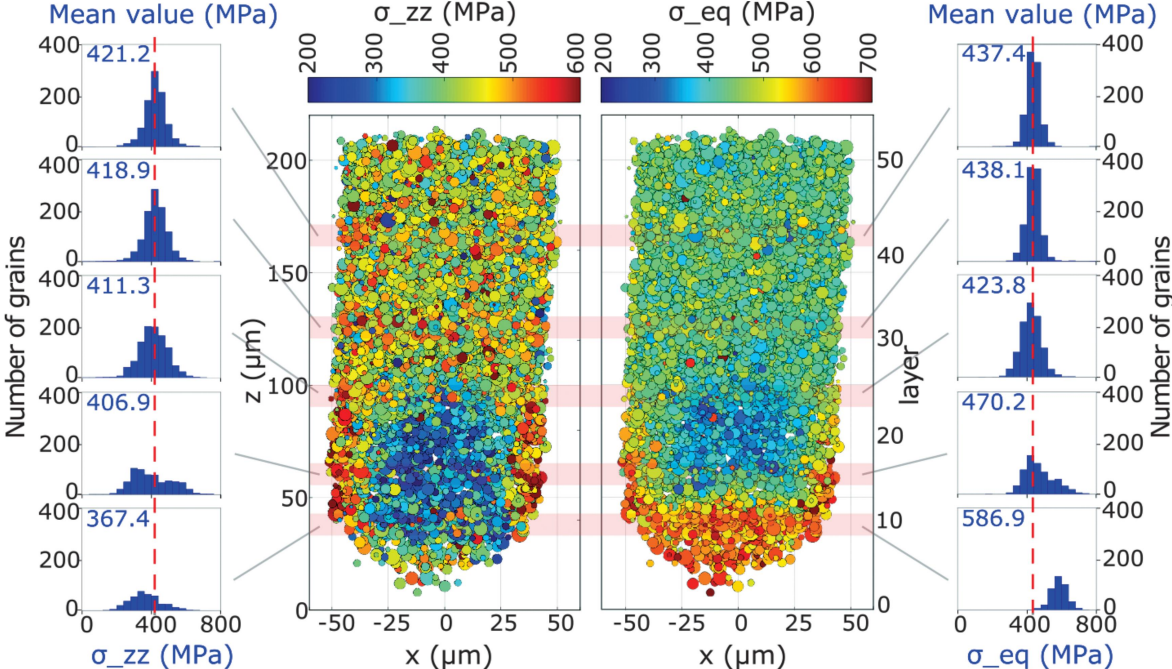


Figure 9: Grain-resolved stresses in austenite, evaluated by the 3D-XRD method, after [35].

Since many other examples than those discussed above are available in the literature, the idea is now to provide the reader with a comprehensive classification of papers on SMAs where full-field measurement techniques are involved. This is the aim of the following section.

4 Classification of the papers found in the literature

We propose in this section a classification of the papers found in the literature, in which the full-field measurement techniques described above are used to characterize SMAs. The Web of Science database¹ was used to identify the papers. **Note that the papers which mention the use of a full-field measurement technique without displaying thermomechanical fields (displacements, strains, temperatures...) are not accounted for in the following tables.**

The reader will first find in Table 1 these references classified according to the type of measurement technique used, alone or in combinations with others. As expected by the two main properties associated with phase transformation in SMAs, namely large deformations and intense heat release/absorption, the two most widely used techniques are DIC and IRT. They are often used in a

¹Web of Science is an online subscription-based scientific citation indexing service managed by Clarivate Analytics, and originally produced by Thomson Scientific’s Institute for Scientific Information (ISI), a division of Thomson Reuters.

complementary manner. The studies reporting the use of DIC are more numerous than those reporting the use of IRT, but it is worth noting that the first publication involving DIC was published after the first publication involving IRT: 2002 and 1997 respectively, see Figures 10-a and -b. The number of studies using DIC increases almost continuously over the years, reaching 26 in 2020. As a general remark, there is a strong diffusion of DIC in the experimental mechanics community, thus explaining this increasing trend for SMA characterization. For IRT, the number of publications has stagnated since the 2010s, with about 10 per year. However, this number can be considered as significant compared to the applications to other types of materials than SMAs. This is certainly due to the strong and localized thermal signature of phase transformations in SMAs, which means that SMAs are "good candidates" for IRT applications. The stagnation of the number of publications using IRT can be explained by a number of pixels that struggles to increase in cooled IR cameras compared to their counterparts designed for the visible domain. It is worth noting that cooled IR cameras exceeding one million of pixels are now available. This should therefore bring a new impetus to the study of SMAs with such tools in the future. It can also be noted that few IRT studies (less than 10%) involve heat source reconstruction (HSR). This approach for processing thermal data should be used more frequently to complement strain measurements, in particular because the use of both types of measurements enables the calculation of energy balances. Figure 10-c shows that MI, GM and 3D-XRD were rarely used. After a few studies in the late 1990s and again in the late 2000s, MI no longer appears in the literature. GM has only been used three times, between 2012 and 2020. These two techniques certainly deserve to be more frequently used because they would bring additional information compared to DIC and IRT, especially thanks to their good compromise between measurement resolution and spatial resolution. **To the best of the authors' knowledge, strain field distributions in the bulk obtained with 3D-XRD are displayed in only two publications.** The limited access to this type of measuring device probably explains this small number. Finally, it is worth noting that Refs [44, 45] mention the use of photoelasticimetry in complement to IRT and DIC+IRT respectively, for the characterization of a composite containing one SMA fiber.

Technique	References
IRT	[46], [47], [48], [49], [50], [51], [52], [53], [54], [55], [56], [44], [57], [58], [45], [59], [60], [61], [62], [63], [64], [65], [66], [67], [68], [69], [70], [71], [72], [73], [74], [75], [76], [77], [78], [79], [80], [81], [82], [83], [84], [40], [43], [85], [86], [87], [88], [89], [90], [91], [92], [36], [93], [94], [95], [96], [97], [98], [99], [100], [101], [102], [103], [104], [105], [106], [107], [108], [109], [110], [111], [112], [113], [114], [115], [116], [117], [118], [119], [120], [121], [122], [123], [124], [125], [126], [127], [128], [129], [130], [131], [132], [133], [134], [135], [136], [137], [138], [139], [140], [141], [142], [143], [144], [145], [146], [147], [148], [149], [150], [151], [152], [153], [154], [155], [156], [157], [158], [159], [37], [160], [161], [162], [163]
DIC	[164], [165], [166], [167], [168], [45], [169], [170], [171], [172], [64], [65], [173], [174], [175], [176], [177], [178], [179], [68], [69], [70], [180], [181], [182], [72], [183], [184], [185], [186], [187], [188], [75], [76], [189], [79], [190], [191], [192], [193], [82], [194], [195], [43], [91], [196], [197], [36], [198], [199], [200], [201], [93], [99], [94], [100], [202], [203], [204], [98], [38], [107], [102], [103], [205], [206], [207], [208], [209], [210], [211], [212], [213], [214], [215], [216], [217], [218], [219], [220], [221], [39], [112], [111], [114], [222], [223], [116], [224], [225], [122], [123], [226], [227], [228], [229], [230], [231], [232], [233], [234], [235], [236], [237], [238], [239], [240], [241], [242], [243], [244], [245], [246], [247], [248], [249], [250], [251], [252], [127], [126], [124], [253], [254], [255], [256], [257], [258], [259], [260], [261], [262], [263], [264], [265], [266], [267], [268], [269], [270], [271], [137], [138], [139], [272], [273], [274], [275], [276], [277], [278], [279], [280], [281], [282], [283], [284], [285], [286], [287], [288], [147], [148], [150], [289], [290], [291], [292], [293], [294], [295], [41], [296], [297], [153], [298], [299], [291], [300], [301], [302], [303], [159], [157], [158], [304], [161], [305], [306], [159], [307], [308], [309], [310], [311], [312]
DIC + IRT	[45], [64], [65], [68], [69], [70], [72], [75], [76], [79], [36], [82], [91], [43], [93], [99], [94], [98], [100], [103], [102], [107], [111], [112], [114], [116], [123], [126], [124], [127], [137], [138], [139], [147], [148], [150], [153], [157], [158], [159], [161]
MI	[313], [42], [314], [315], [316], [317], [318], [319], [53], [56], [320], [321], [322], [323], [324], [325]
GM	[40], [326], [327]
GM + IRT	[40]
IRT with HSR	[48], [58], [65], [70], [72], [84], [40], [43], [110], [146], [154], [37], [158]
3D-XRD	[35], [271]

Table 1: Classification by type of measurement technique. In each box of the table, the references are listed in chronological order. IRT: InfraRed Thermography, DIC: Digital Image Correlation, GM: Grid Method, MI: Moiré Interferometry, HSR: Heat Source Reconstruction.

Table 2 gives the list of references according to the chemical elements of the tested SMA. The monocrystalline or polycrystalline character is also reported. Multi-crystals (containing a few grains) are gathered with single-crystals. As expected, most of the studies described in the literature concern polycrystalline NiTi specimens, so this table provides the references only for the other types. Polycrystalline NiTi SMAs being the most widely used in engineering applications because of their biocompatibility, their stability and the possibility of tuning their properties by cold working and heat treatment, they are the most widely studied with full-field measurement techniques. It is however quite surprising to note that copper-based SMAs are not so much studied despite their use in a variety of existing or promising applications such as damping devices or elastocaloric systems. For NiTi alloys, only two references concern single-crystals, which is to be compared to the about 200 references found for their polycrystalline counterparts. The trend is opposite for NiTiHf: five references among eight deal with single-crystals for this type of alloy. Single-crystal copper-based alloys are also more studied than polycrystalline ones but the total number of studies for these alloys is small. Studies (in small numbers) on single-crystals exist for other types of alloys, as also shown in the table. Single-crystals should however be more widely studied in the future because they potentially give more insight into

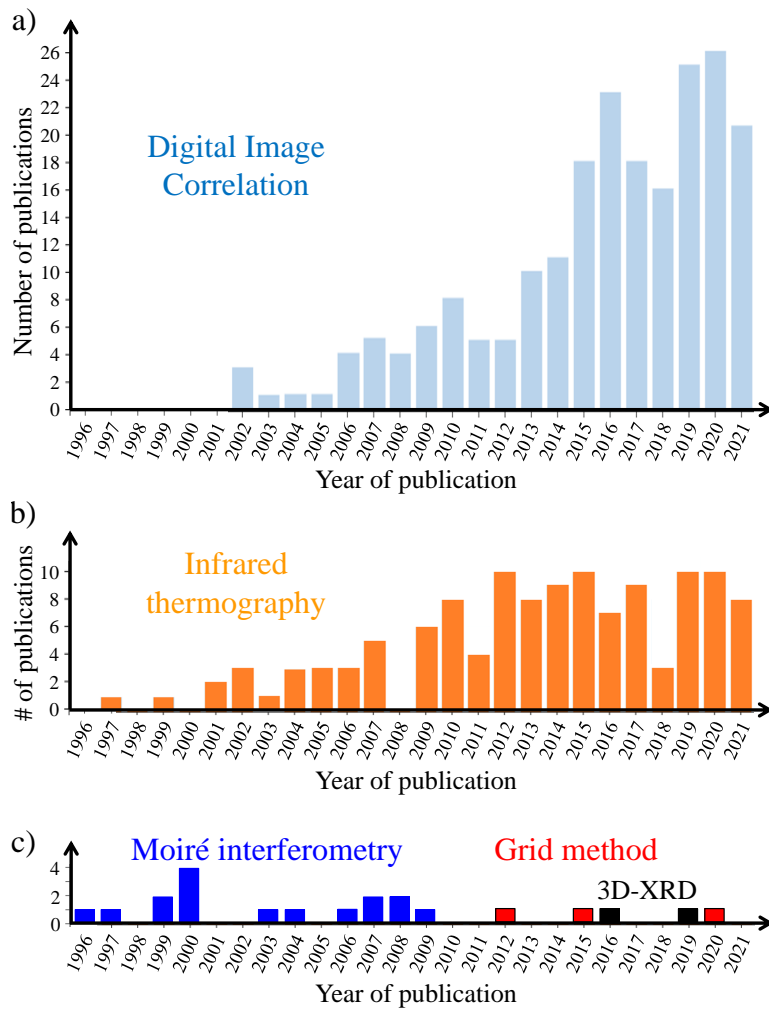


Figure 10: Number of papers on SMAs over the years involving a) DIC, b) IRT and c) MI, GM and 3D-XRD.

the understanding of martensitic microstructures than polycrystals. Besides, small-scale measurements (allowing access to microstructures within grains) are also promising to build relevant macroscopic behavior models for polycrystals. It can be noted that there is only a few studies on areas smaller than 1 mm^2 , see Table 3 which gives the classification of the publications with respect to the size of the region of interest. In this table, it can also be noted that most of the references correspond to an observation of areas smaller than 100 mm^2 , which can be considered as small compared to full-field measurement studies dealing with other types of materials such as non-active ones. This is due to the fact that many studies on SMAs are carried out on NiTi wires whose diameter seldom exceeds a few millimeters, which penalizes measurements on long specimens. The use of new cooled IR cameras with sensors featuring more than one million pixels should allow to increase the length of the wires or cables under study, which should be beneficial for engineering applications.

Alloy	Single-crystal or multicrystal	Polycrystal
FeAl	[219]	
FeGa		[220]
FeGaB		[220]
FeMnNiAl		[294], [310]
FeMnSiCr	[323]	
FeMnSiCrNi		[137]
CoNiAl	[190], [111]	
CoNiGa	[188], [129]	[298]
CuAlMn	[297], [161], [311]	[152]
CuZnAl	[48], [53], [58], [81], [327]	[313]
CuAlNi	[42], [314], [315], [318], [316], [89], [201], [154]	[63]
CuAlBe	[72], [181], [186], [77], [189], [84], [40], [326]	[164], [62], [178], [184]
NiFeGa	[177], [111]	[83]
NiFeGaCo	[109]	
NiMnGa	[171], [176], [192], [203], [207], [237], [265], [266]	
NiMnTi		[139]
NiCoMnTi		[139], [147]
NiMnInCu		[130]
NiMnSn	[138]	[131]
NiTiCo		[141]
NiTiCu		[88]
NiTiCuCo		[226]
NiTiFe		[124]
NiTiNb		[328], [215], [243], [293], [292], [290], [301]
NiTiHf	[228], [230], [231], [245], [247]	[214], [223], [284]
NiTi	[179], [111]	Others

Table 2: Classification by type of alloy.

Size S in mm^2	References
$S > 100$	[313], [50], [51], [167], [44], [56], [45], [57], [170], [61], [60], [169], [171], [173], [65], [64], [174], [62], [324], [70], [71], [72], [183], [69], [77], [74], [75], [76], [80], [79], [191], [84], [194], [43], [91], [40], [87], [86], [85], [199], [93], [201], [202], [95], [94], [100], [99], [106], [38], [208], [101], [103], [105], [39], [110], [326], [211], [212], [112], [215], [222], [227], [118], [122], [123], [119], [225], [235], [236], [240], [241], [249], [127], [254], [132], [261], [135], [140], [137], [145], [148], [273], [275], [149], [151], [327], [292], [295], [156], [153], [155], [300], [303], [160], [163]
$1 < S < 100$	[46], [42], [314], [47], [315], [318], [319], [316], [317], [48], [49], [52], [164], [165], [166], [54], [53], [168], [55], [58], [169], [59], [172], [321], [66], [175], [63], [174], [176], [324], [177], [179], [178], [181], [68], [325], [184], [182], [67], [71], [185], [73], [329], [78], [186], [190], [189], [187], [188], [195], [83], [81], [36], [192], [82], [89], [88], [196], [90], [92], [98], [97], [198], [96], [204], [200], [93], [94], [203], [207], [104], [38], [102], [205], [213], [221], [209], [210], [214], [330], [216], [219], [220], [108], [221], [109], [111], [113], [218], [114], [115], [223], [116], [121], [228], [234], [237], [239], [120], [232], [233], [230], [231], [226], [117], [243], [242], [245], [247], [250], [251], [129], [246], [124], [248], [252], [125], [244], [128], [130], [131], [253], [255], [256], [257], [258], [133], [134], [262], [264], [265], [266], [259], [267], [268], [269], [270], [271], [140], [141], [136], [142], [144], [274], [278], [279], [280], [139], [277], [143], [281], [282], [283], [285], [286], [287], [284], [293], [276], [150], [294], [297], [147], [296], [146], [291], [289], [290], [153], [288], [298], [154], [301], [302], [303], [304], [307], [37], [157], [306], [161], [305], [312], [159], [158], [308], [309], [310], [162], [163], [311]
$0.1 < S < 1$	[314], [316], [323], [200], [206], [107], [210], [224], [219], [231], [126], [263], [152], [41]
$0.01 < S < 0.1$	[320], [217], [229], [260], [272]
$S < 0.01$	[320], [322], [193], [238], [35], [263], [281], [299], [308]

Table 3: Classification by size of the zone observed by full-field measurement technique. In each box of the table, the references are listed in chronological order.

Before concluding, the reader can find in Tables 4 and 5 a classification of the publications according to the sample geometry and the type of loading. It can be seen in the first table that most of the publications concerns stress-induced transformation, *i.e.* under mechanical loading. This can be explained by the fact that managing a thermal loading while performing a measurement by camera is more complex to achieve than applying a mechanical loading at constant room temperature. Besides, a temperature-induced transformation leads to a "modification" of the thermal loading due to the production/absorption of latent heat (heat production during cooling and heat absorption during heating), this making complex the analysis of the results. **It can also be seen that only two references concern the use of a magnetic excitation. It was for a magnetic NiMnGa single-crystal. In practice, the authors performed DIC under magneto-thermo-mechanical loading, namely cyclic magnetic field, constant compression load and variable heat exchange conditions.**

Table 5 focuses on some specific types of mechanical loadings. It shows that there is a wide range of specimen geometries and types of tests discussed in the literature for which full-field measurement systems have been used.

5 Conclusion and suggestions for future work

This review on the use of full-field surface measurement techniques for SMA characterization clearly shows that these techniques have gained popularity in the recent years. Their ability to reveal rich microstructures which appear in SMA specimens during thermomechanical tests, and the fact that various commercial codes are available for some of these techniques, certainly explain this success.

The classification proposed in this paper indicates that a wide range of materials, techniques, tests and specimen geometries are concerned by these techniques. An important point which should be underlined is that full-field measurement techniques are not yet stabilized, in the sense that their development should be seen as an evolutionary process. This is illustrated by the fact that no standard is currently available to calibrate these systems and assess their metrological performance in a common and unified way. In the same way, the number of pixels of camera sensors, both in the visible and infrared range, is steadily increasing. The same remark holds for the performance of computers in terms of speed and memory size. Future results will certainly involve larger image sizes and image processing techniques leading to a better compromise between measurement and spatiotemporal resolutions. We can also expect that artificial intelligence will bring new post-processing tools. In conclusion, we would like to highlight the following topics, which certainly deserve dedicated studies in the near future:

- Techniques such as those suitable for strain and temperature measurements have already been coupled in some studies. This approach should certainly be rolled out in a more systematic way, in particular because such techniques offer complementary information, thus enabling the experimentalists to carry out energy balance for instance;
- Displacement and strain fields are generally obtained with DIC, which relies on a random marking of the surfaces of interest. However, it has been shown that using periodic patterns processed with a spectral method gives a better compromise between spatial and measurement resolutions, which is crucial for a better characterization of sharp details in strain maps. Such techniques therefore deserve to be used more frequently when complex microstructures are to be characterized;
- Displacement and strain measurements are often performed along one direction only, for instance the longitudinal direction for a uniaxial tensile test, while full-field measurement systems generally provide the three in-plane components at the surface of the specimen. These three components should be more often taken into account in the analysis of the results obtained;
- Despite the richness of the information provided by 3D X-ray diffraction, **very few papers involving this technique for measurements in the bulk have been found in this review. 3D-XRD can be used to obtain various quantities such as crystallographic orientation fields, but the measurement of strain fields has only been seldom performed for the analysis of phase transformation in SMAs;**
- Temperature changes are often used as primary quantities to analyze phase changes in SMAs. It is however now well established that such quantities are prone to parasitic effects, while heat sources provide reliable information about the heat signature of various mechanical phenomena. Experimentalists using IR thermography should therefore bear in mind this possibility, the price

to pay being to extract heat source maps from temperature change distributions by using a suitable image processing technique relying on the heat equation;

- Single-crystal specimens are more difficult to get from suppliers than polycrystal ones. However, they give access to the "elementary" microstructures which are at the basis of many SMA properties. They should therefore be considered with more attention when using full-field measurement techniques;
- Moiré interferometry seems to have nearly disappeared in the most recent papers reported in this study. This is probably a consequence of the popularity and improved ease of use of DIC. Yet, moiré interferometry still remains incomparable to reveal sharp details in microstructures at the microscale;
- **Most of the publications concern the use of full-field measurement techniques to investigate the stress-induced transformation at ambient temperature. It would also be of interest to further study the temperature-induced transformation as well as the magnetic field-induced transformation (for magnetic SMAs) with full-field measurement techniques;**
- Finally, too few studies deal with strain measurements at the microscale. SMA researchers should be aware of that some full-field measurement techniques are adaptable to the microscale with some caution. They provide in this case valuable information to understand mechanisms occurring at the grain level of polycrystals.

	Thermal loading (temperature-induced transformation)	Mechanical loading (stress-induced transformation, superelastic/pseudoelastic cycles)	Magnetic loading
Wire/fiber	[165], [54], [238], [260], [292]	[47], [317], [50], [52], [166], [167], [168], [55], [59], [66], [68], [73], [36], [92], [101], [108], [113], [115], [35], [238], [120], [128], [125], [126], [134], [260], [274], [141], [272], [144], [152], [154], [151], [148], [146], [299], [301], [37], [159], [158], [160], [162]	
Rod		[205], [147], [312]	
Cylindrical bar		[182], [221], [298], [312]	
Cable		[93], [94], [106], [119]	
Tube		[49], [65], [64], [70], [195], [196], [38], [208], [121], [123], [273], [296], [304]	
Film/foil	[207]	[172], [185], [88], [96], [102], [114], [116], [226], [124], [280]	
Strip		[317], [51], [56], [57], [60], [61], [74], [80], [86], [85], [90], [95], [97], [105], [112], [248], [132], [140], [142], [83]	
Plate/sheet	[319], [170], [100], [110]	[169], [173], [62], [179], [183], [184], [71], [72], [186], [329], [77], [84], [194], [197], [87], [40], [43], [39], [326], [246], [133], [263], [278], [137], [136], [143], [275], [149], [300], [303], [309]	
Prismatic	[265], [266]	[313], [164], [53], [171], [320], [321], [176], [325], [188], [190], [192], [202], [203], [108], [109], [214], [219], [220], [223], [228], [230], [234], [237], [242], [245], [129], [256], [270], [265], [266], [271], [139], [297], [161], [311]	[265], [266]
Cylindrical dog-bone		[48], [58], [81], [213], [268], [283]	
Flat dog-bone	[216], [227], [231], [247]	[42], [46], [314], [315], [316], [318], [174], [177], [323], [178], [181], [79], [75], [76], [189], [78], [187], [193], [82], [91], [89], [99], [204], [98], [202], [201], [198], [104], [103], [111], [217], [216], [219], [111], [222], [227], [229], [230], [231], [233], [234], [235], [236], [225], [122], [241], [242], [244], [245], [247], [251], [252], [254], [255], [256], [257], [261], [262], [259], [135], [267], [277], [279], [282], [285], [287], [41], [150], [291], [294], [295], [327], [153], [156], [155], [291], [302], [157], [306], [308], [163], [312]	
Particles in composite		[258]	
Fibers in composite	[44], [45], [215], [290], [293]	[328], [118], [117], [249], [159],	
Ring	[243]		
Notched plate	[240]	[173], [174], [175], [324], [182], [67], [191], [200], [206], [107], [209], [210], [224], [218], [232], [236], [239], [240], [127], [248], [249], [250], [253], [264], [258], [269], [276], [281], [145], [284], [286], [294], [153], [307], [306]	
Meuwissen specimen		[199], [211], [212]	
Diamond shape		[289], [305]	
Porous SMA	[320], [322]		
3D printed		[234], [288], [304], [310]	

Table 4: Classification by type of specimen, with a distinction between thermal, mechanical and magnetic loadings.

	Mechanical fatigue	Thermal fatigue	Bending	Torsion	Compression	Pure shear	Multi-axial loading	Impact/Buckling	Cracking
Wire/fiber	[47], [50], [101], [113], [120], [238], [126], [141], [158]	[54], [238]	[168], [134], [299], [162]	[125]	[160]			[148]	
Rod			[205]		[147], [205]			[312]	[205]
Cylindrical bar					[221], [298]	[304]	[221]		
Tube	[121]		[195], [38], [205], [208], [273]	[196], [38], [205], [208], [304]		[196], [123], [296]		[205], [273]	
Strip	[105]					[51]	[56]		
Plate/sheet	[87]		[136], [300]			[71], [202]	[69], [194], [263]	[149]	[197]
Prismatic specimen	[311]	[63]	[313]	[165]	[53], [176], [325], [190], [192], [83], [109], [214], [219], [220], [223], [228], [230], [234], [131], [130], [242], [245], [256], [265], [266], [139], [297], [161]		[164], [203]		[171]
Cylindrical dog-bone					[213]		[213]		
Flat dog-bone	[76], [204], [241], [252], [254], [257], [261], [135], [277], [282], [287], [150], [155], [163]	[247]					[262]		
Fibers in composite								[151]	
Particles in composite									[258]
Notched plate	[253], [269], [286], [276]	[240]			[182]				[175], [107], [232], [127], [276], [145], [153]
Meuwissen specimen					[199], [211], [212]				
3D printed				[304]	[234], [310]	[304]			

Table 5: Classification by type of specimen and type of test (apart from the classical tensile test).

References

- [1] Pierron, F. and Grédiac, M. “Towards Material Testing 2.0. A review of test design for identification of constitutive parameters from full-field measurements”. In: *Strain* 57 (2021), e12370.
- [2] Roux, S., Besnard, G. and Hild, F. “Finite-Element Displacement Fields Analysis from Digital Images: Application to Portevin-Le Châtelier Bands”. In: *Exp. Mech.* 46 (2006), pp. 789–803.
- [3] Pan, B., Qian, K., Xie, H. and Asundi, A. “Two-dimensional digital image correlation for in-plane displacement and strain measurement: a review”. In: *Meas. Sci. Technol.* 20 (2009), p. 062001.
- [4] Wittevrongel, L., Lava, P., Lomov, S. V. and Debruyne, D. “A Self Adaptive Global Digital Image Correlation Algorithm”. In: *Exp. Mech.* 55 (2015), pp. 361–378.
- [5] Kammers, A. and Daly, S. “Small-scale patterning methods for digital image correlation under scanning electron microscopy”. In: *Meas. Sci. Technol.* 22 (2011), p. 125501.
- [6] Kammers, A. and Daly, S. “Digital Image Correlation under Scanning Electron Microscopy: Methodology and Validation”. In: *Exp. Mech.* 53 (2013), pp. 1743–1761.
- [7] Kammers, A. and Daly, S. “Self-Assembled Nanoparticle Surface Patterning for Improved Digital Image Correlation in a Scanning Electron Microscope”. In: *Exp. Mech.* 53 (2013), pp. 1333–1341.
- [8] Weidner, A. and Biermann, H. “Review on Strain Localization Phenomena Studied by High-Resolution Digital Image Correlation”. In: *Adv. Eng. Mater.* 23 (2021), p. 2001409.
- [9] Grédiac, M., Blaysat, B. and Sur, F. “A critical comparison of some metrological parameters characterizing local Digital Image Correlation and Grid Method”. In: *Exp. Mech.* 57 (2017), pp. 871–903.
- [10] Grédiac, M., Sur, F. and Blaysat, B. “Comparing several spectral methods used to extract displacement and strain fields from checkerboard images”. In: *Opt. Lasers Eng.* 127 (2020), p. 105984.
- [11] Reu, P., Blaysat, B., Jones, E., Iadicola, M., Fayad, S., Toussaint, E., Lava, P., Rethore, J., Yang, J., Bhattacharya, K., Yang, L., Deb, D., Vemulapati, C., Klein, M., Ando, E., Roubin, E., Stamati, O., Couture, C., Landauer, A., Liu, M., Turner, D., Jaminion, S., Siebert, T. and Olufsen, S. “DIC Challenge: Developing Images and Guidelines for Evaluating Accuracy and Resolution of 2D Analyses. Focus on the Metrological Efficiency Indicator”. In: *Exp. Mech.* (2021). Submitted.
- [12] Sutton, M., Orteu, J. and Schreier, H. *Image Correlation for Shape, Motion and Deformation Measurements: Basic Concepts, Theory and Applications*. Springer-Verlag New York Inc., 2009.
- [13] Bomarito, G., Hochhalter, J., Ruggles, T. and Cannon, A. “Increasing accuracy and precision of digital image correlation through pattern optimization”. In: *Opt. Lasers Eng.* 91 (2017), pp. 73–85.
- [14] Fayad, S., Seidl, D. and Reu, P. “Spatial DIC Errors due to Pattern-Induced Bias and Grey Level Discretization”. In: *Exp. Mech.* 60 (2020), pp. 249–263.
- [15] Sur, F., Blaysat, B. and Grédiac, M. “On biases in displacement estimation for image registration, with a focus on photomechanics”. In: *J. Math. Imaging Vision* (2020). Accepted, online.
- [16] Grédiac, M., Blaysat, B. and Sur, F. “Extracting displacement and strain fields from checkerboard images with the Localized Spectrum Analysis”. In: *Exp. Mech.* 59 (2019), pp. 207–218.
- [17] Grédiac, M., Blaysat, B. and Sur, F. “On the optimal pattern for displacement field measurement: random speckle and DIC, or checkerboard and LSA?” In: *Exp. Mech.* 60 (2020), pp. 509–534.

- [18] Grédiac, M., Sur, F. and Blaysat, B. “Removing Quasi-Periodic Noise in Strain Maps by Filtering in the Fourier Domain”. In: *Exp. Tech.* 40 (2016), pp. 959–971.
- [19] Mirmohammad, H. and Kingstedt, O. “Theoretical Considerations for Transitioning the Grid Method Technique to the Microscale”. In: *Exp. Mech.* 61 (2021), pp. 753–770.
- [20] Piro, J. and Grédiac, M. “Producing and Transferring Low-Spatial-Frequency Grids for Measuring Displacement Fields with moiré and Grid Methods”. In: *Exp. Tech.* 28 (2004), pp. 23–26.
- [21] Surrel, Y. *Images optiques; mesures 2D et 3D*. Conservatoire National des Arts et Métiers, Paris, France. 2003.
- [22] Post, D., Han, B. and Ifju, P. *High Sensitivity Moiré. Experimental analysis for mechanical and materials*. Springer-Verlag New York, 1994.
- [23] Surrel, Y. “Les techniques optiques de mesure de champ: essai de classification”. In: *Instr. Mes. Metrol.* 5.1–2 (2005).
- [24] Jacquot, P. “Speckle Interferometry: A Review of the Principal Methods in Use for Experimental Mechanics Applications”. In: *Strain* 44 (2008), pp. 57–69.
- [25] Asundi, A. “Moiré interferometry for deformation measurement”. In: *Opt. Lasers Eng.* 11 (1989), pp. 281–292.
- [26] Vollmer, M. and Mollman, K. *Infrared Thermal Imaging: Fundamentals, Research and Applications, Second edition*. Wiley-VCH Verlag GmbH, 2018.
- [27] Batsale, J., Chrysochoos, A., Pron, H. and Wattrisse, B. “Thermographic Analysis of Material Behavior”. In: *Full-Field Measurements and Identification in Solid Mechanics*. Ed. by M. Grédiac and F. Hild. Vol. 16. Wiley-ISTE, 2012, pp. 439–468.
- [28] Jing, Y., Laurent, F., Stéphane, A. and Alain, N. “A numerical study of heat source reconstruction for the advection diffusion operator: a conjugate gradient method stabilized with SVD”. In: *Int. J. Therm. Sci.* 104 (2016), pp. 68–85.
- [29] Chrysochoos, A. and Louche, H. “An infrared image processing to analyse the calorific effects accompanying strain localisation”. In: *Int. J. Eng. Sci.* 38 (2000), pp. 1759–1788.
- [30] Poulsen, H., Lauridsen, S. N. E., Schmidt, S., Suter, R., Lienert, U., Margulies, L., Lorentzen, T. and Jensen, D. “Three-dimensional maps of grain boundaries and the stress state of individual grains in polycrystals and powders”. In: *J. Appl. Crystallogr.* 34 (2001), pp. 751–756.
- [31] Korsunsky, A., Vorster, W., Zhang, S., Dini, D., Latham, D., Golshan, M., Liu, J., Kyriakoglou, Y. and Walsh, M. “The principle of strain reconstruction tomography: Determination of quench strain distribution from diffraction measurements”. In: *Acta Mater.* 54 (2006), pp. 2101–2108.
- [32] Hayashi, Y., Hirose, Y. and Seno, Y. “Polycrystal orientation mapping using scanning three-dimensional X-ray diffraction microscopy”. In: *J. Appl. Crystallogr.* 48 (2015), pp. 1094–1101.
- [33] Hektor, J., Hall, S., Henningsson, N., Engqvist, J., Ristinmaa, M., Lenrick, F. and Wright, J. “Scanning 3DXRD Measurement of Grain Growth, Stress, and Formation of Cu₆Sn₅ around a Tin Whisker during Heat Treatment”. In: *Materials* 12 (2019), p. 446.
- [34] Henningsson, N., Hall, S., Wright, J. and Hektor, J. “Reconstructing intragranular strain fields in polycrystalline materials from scanning 3DXRD data”. In: *J. Appl. Crystallogr.* 53 (2020), pp. 314–325.
- [35] Sedmák, P., Pilch, J., Heller, L., Kopeček, J., Wright, J., Sedlák, P., Frost, M. and Šittner, P. “Grain-resolved analysis of localized deformation in nickel-titanium wire under tensile load”. In: *Science* 353 (2016), pp. 559–562.
- [36] Reedlunn, B., Daly, S., Hector, L., Zavattieri, P. and Shaw, J. “Tips and Tricks for Characterizing Shape Memory Wire Part 5 : Full-Field Strain Measurement by Digital Image Correlation”. In: *Exp. Tech.* 37 (2013), pp. 62–78.

- [37] Jury, A., Balandraud, X., Heller, L., Šittner, P. and Karlik, M. “Reconstruction of Heat Sources Induced in Superelastically Loaded Ni-Ti Wire By Localized Deformation Processes”. In: *Exp. Mech.* 61 (2021), pp. 349–366.
- [38] Reedlunn, B., Churchill, C. B., Nelson, E. E., Shaw, J. A. and Daly, S. H. “Tension, compression, and bending of superelastic shape memory alloy tubes”. In: *J. Mech. Phys. Solids* 63 (2014), pp. 506–537.
- [39] Xiao, Y., Zeng, P., Lei, L. and Du, H. “Local Mechanical Response of Superelastic NiTi Shape-Memory Alloy Under Uniaxial Loading”. In: *Shap. Mem. Superelasticity* 1 (2015), pp. 468–478.
- [40] Delpueyo, D., Grédiac, M., Balandraud, X. and Badulescu, C. “Investigation of martensitic microstructures in a monocrystalline Cu-Al-Be shape memory alloy with the grid method and infrared thermography”. In: *Mech. Mater.* 45 (2012), pp. 34–51.
- [41] Polatidis, E., Smid, M., Kubena, I., Hsu, W., Laplanche, G. and Van Swygenhoven, H. “Deformation mechanisms in a superelastic NiTi alloy: An in-situ high resolution digital image correlation study”. In: *Mater. Des.* 191 (2020), p. 108622.
- [42] Zhang, X., Xu, T., Sun, Q. and Tong, P. “On the Full-Field Deformation of Single Crystal CuAlNi Shape Memory Alloys Stress-Induced $\beta(1) \rightarrow \gamma'(1)$ Martensitic Transformation”. In: *J. Phys. IV* 7.C5 (1997), pp. 555–560.
- [43] Louche, H., Schlosser, P., Favier, D. and Orgéas, L. “Heat Source Processing for Localized Deformation with Non-Constant Thermal Conductivity. Application to Superelastic Tensile Tests of NiTi Shape Memory Alloys”. In: *Exp. Mech.* 52 (2012), pp. 1313–1328.
- [44] Murasawa, G., Yoneyama, S., Tohgo, K. and Takashi, M. “Distribution of unique performances for shape memory alloy composite”. In: *Advances in Nondestructive Evaluation, PT 1-3*. Ed. by S. Lee, D. Yoon, J. Lee and S. Lee. Vol. 270–273. Key Engineering Materials. Trans Tech Publications Ltd, Zurich, Switzerland, 2004, pp. 2172–2178.
- [45] Murasawa, G. “Analytical model for predicting internal stress and deformation of shape memory alloy composite”. In: *Smart Structures and Materials 2005: Active Materials: Behavior and Mechanics*. Ed. by W. Armstrong. Vol. 5761. Proceedings of SPIE. SPIE-Int. Soc. Optical Engineering, Bellingham, USA, 2005, pp. 395–405.
- [46] Shaw, J. and Kyriakides, S. “On the nucleation and propagation of phase transformation fronts in a NiTi alloy”. In: *Acta Mater.* 45 (1997), pp. 683–700.
- [47] Tobushi, H., Nakahara, T., Shimeno, Y., T. and Hashimoto. “Low-Cycle Fatigue of TiNi Shape Memory Alloy and Formulation of Fatigue Life”. In: *ASME. J. Eng. Mater. Technol.* 122 (1999), pp. 186–191.
- [48] Balandraud, X., Chrysochoos, A., Leclercq, S. and Peyroux, R. “Influence of the thermomechanical coupling on the propagation of a phase change front”. In: *C. R. Acad. Sci. - Ser. IIB - Mech.* 329 (2001), pp. 621–626.
- [49] Helm, D. and Haupt, P. “Thermomechanical behavior of shape memory alloys”. In: *Smart Structures and Materials 2001: Active Materials: Behavior and Mechanics*. Ed. by C. Lynch. Vol. 4333. Proceedings of the Society of Photo-Optical Instrumentation Engineers (SPIE). SPIE-Int. Soc. Optical Engineering, Bellingham, USA, 2001, pp. 302–313.
- [50] Iadicola, M. and Shaw, J. A. “The effect of uniaxial cyclic deformation on the evolution of phase transformation fronts in pseudoelastic NiTi wire”. In: *J. Intell. Mater. Syst. Struct.* 13 (2002), pp. 143–155.
- [51] Gadaj, S., Nowacki, W. and Pieczyska, E. “Temperature evolution in deformed shape memory alloy”. In: *Infrared Phys. Technol.* 43 (2002), pp. 151–155.

- [52] Iadicola, M. and Shaw, J. “An Experimental Setup for Measuring Unstable Thermo-Mechanical Behavior of Shape Memory Alloy Wire”. In: *J. Intell. Mater. Syst. Struct.* 13 (2002), pp. 157–166.
- [53] Lu, R. and Fang, R. “Compressive response of CuAlNi single crystal”. In: *Optical Technology and Image Processing for Fluids and Solids Diagnostics 2002*. Ed. by G. Shen, S. Cha, F. Chiang and C. Mercer. Vol. 5058. Proceedings of the Society of Photo-Optical Instrumentation Engineers (SPIE). SPIE-Int. Soc. Optical Engineering, Bellingham, USA, 2002, pp. 633–637.
- [54] Ng, Y., Song, C., McLean, D., Shimi, S. M., Frank, T. G., Cuschieri, A. and Campbell, P. A. “Optimized deployment of heat-activated surgical staples using thermography”. In: *Appl. Phys. Lett.* 83 (2003), pp. 1884–1886.
- [55] Iadicola, M. and Shaw, J. “Rate and thermal sensitivities of unstable transformation behavior in a shape memory alloy”. In: *Int. J. Plast.* 20 (2004), pp. 577–605.
- [56] Turner, T., Buehrle, R., Cano, R. and Flemings, G. “Design, fabrication, and testing of SMA enabled adaptive chevrons for jet noise reduction”. In: *Smart Structures and Materials 2004: Smart Structures and Integrated Systems*. Ed. by A. Flatau. Vol. 5390. Proceedings of the Society of Photo-optical Instrumentation Engineers (SPIE). SPIE-Int. Soc. Optical Engineering, Bellingham, USA, 2004, pp. 297–308.
- [57] Gadaj, S., Nowacki, W., Pieczyska, E. and Tobushi, H. “Temperature measurement as a new technique applied to the phase transformation study in a TiNi shape memory alloy subjected to tension”. In: *Arch. Metall. Mater.* 50 (2005), pp. 661–674.
- [58] Chrysochoos, A., Licht, C. and Peyroux, R. “Propagation of phase change front in monocrystalline SMA”. In: *Mechanical Modelling and Computational Issues in Civil Engineering*. Ed. by M. Fremond and F. Marceri. Vol. 23. Lectures Notes in Applied and Computational Mechanics. Springer-Verlag Berlin Heidelberg, 2005, pp. 369–377.
- [59] Chang, B., Shaw, J. and Iadicola, M. “Thermodynamics of Shape Memory Alloy Wire: Modeling, Experiments, and Application”. In: *Continuum Mech. Thermodyn.* 18 (2006), pp. 83–118.
- [60] Pieczyska, E. A., Gadaj, S. P., Nowacki, W. K. and Tobushi, H. “Phase-Transformation Fronts Evolution for Stress- and Strain-Controlled Tension Tests in TiNi Shape Memory Alloy”. In: *Exp. Mech.* 46 (2006), pp. 531–542.
- [61] Pieczyska, E. A., Tobushi, H., Gadaj, S. and Nowacki, W. “Superelastic Deformation Behaviors Based on Phase Transformation Bands in TiNi Shape Memory Alloy”. In: *Mater. Trans.* 47 (2006), pp. 670–676.
- [62] Vieille, B., Michel, J., Boubakar, M. and LExcellent, C. “Validation of a 3D numerical model of shape memory alloys pseudoelasticity through tensile and bulging tests on CuAlBe sheets”. In: *Int. J. Mech. Sci.* 49 (2007), pp. 280–297.
- [63] Seiner, H., Landa, M. and Sedlák, P. “Propagation of an austenite-martensite interface in a thermal gradient”. In: *Proc. Est. Acad. Sci. Phys. Math.* 56 (2007), pp. 218–225.
- [64] Favier, D., Louche, H., Schlosser, P., Orgéas, L., Vacher, P. and Debove, L. “Homogeneous and heterogeneous deformation mechanisms in an austenitic polycrystalline Ti-50.8at.% Ni thin tube under tension. Investigation via temperature and strain fields measurements”. In: *Acta Mater.* 55 (2007), pp. 5310–5322.
- [65] Schlosser, P., Louche, H., Favier, D. and Orgéas, L. “Image processing to estimate the heat sources related to phase transformations during tensile test of NiTi tubes”. In: *Strain* 43 (2007), pp. 260–271.
- [66] Iadicola, M. A. and Shaw, J. A. “An experimental method to measure initiation events during unstable stress-induced martensitic transformation in a shape memory alloy wire”. In: *Smart Mater. Struct.* 16 (2007), S155–S169.

- [67] Gollerthan, S., Young, M., Neuking, K., Ramamurty, U. and Eggeler, G. “Direct physical evidence for the back-transformation of stress-induced martensite in the vicinity of cracks in pseudoelastic NiTi shape memory alloys”. In: *Acta Mater.* 57 (2009), pp. 5892–5897.
- [68] Churchill, C. B., Shaw, J. A. and Iadicola, M. A. “Tips and tricks for characterizing shape memory alloy wire: Part 3-localization and propagation phenomena”. In: *Exp. Tech.* 33 (2009), pp. 70–78.
- [69] Grolleau, V., Louche, H., Penin, A., Chauvelon, P., Rio, G., Liu, Y. and Favier, D. “Bulge tests on ferroelastic and superelastic NiTi sheets with full field thermal and 3D-kinematical measurements : experiments and modelling”. In: *ESOMAT 2009 - 8th European Symposium on Martensitic transformations*. Ed. by P. Sittner, V. Paidar, L. Heller and H. Seiner. EDP Sciences, 2009, p. 06011.
- [70] Schlosser, P., Favier, D., Louche, H., Orgéas, L. and Liu, Y. “From the thermal and kinematical full-field measurements to the analysis of deformation mechanisms of NiTi SMAs”. In: *ESOMAT 2009 - 8th European Symposium on Martensitic transformations*. Ed. by P. Sittner, V. Paidar, L. Heller and H. Seiner. EDP Sciences, 2009, p. 06010.
- [71] Pieczyska, E., Gadaj, S., Luckner, J., Nowacki, W. and Tobushi, H. “Martensite and Reverse Transformation during Complete Cycle of Simple Shear of NiTi Shape Memory Alloy”. In: *Strain* 45 (2009), pp. 93–100.
- [72] Vigneron, S., Chrysochoos, A., Peyroux, R. and Wattrisse, B. *Analyse énergétique de la localisation du changement de phase dans un AMF monocristallin*. Congrès Français de Mécanique, 24-28 August 2009, Marseille, France. 2009.
- [73] Churchill, C. B., Shaw, J. A. and Iadicola, M. A. “Tips and tricks for characterizing shape memory alloy wire: Part 4 - Thermo-mechanical coupling”. In: *Exp. Tech.* 34 (2010), pp. 63–80.
- [74] Pieczyska, E. and Tobushi, H. “Infrared imaging of TiNi shape memory alloy subjected to deformation at various temperatures”. In: *ICEM 14: 14th International Conference on Experimental Mechanics, Vol 6*. Ed. by F. Bremand. EDP Sciences, 2010, p. 29009.
- [75] Saletti, D., Pattofatto, S. and Zhao, H. “Evolution of the martensitic transformation in shape memory alloys under high strain rates”. In: *ICEM 14: 14th International Conference on Experimental Mechanics, Vol 6*. Ed. by F. Bremand. EDP Sciences, 2010, p. 29008.
- [76] Kim, K., Juggernaut, K. and Daly, S. “Stress-Induced Martensitic Phase Transformation in Nitinol Under Hard Cyclic Loading”. In: *ASME 2010 Conference on Smart Materials, Adaptive Structures and Intelligent Systems*. Vol. 1. Smart Materials, Adaptive Structures and Intelligent Systems. 2010, pp. 1–7.
- [77] Delpueyo, D., Balandraud, X., Grédiac, M. and Fillit, R. “Thermoelastic analysis of a copper-based monocristalline shape-memory alloy”. In: *ICEM 14: 14th International Conference on Experimental Mechanics, Vol 6*. Ed. by F. Bremand. EDP Sciences, 2010, p. 29007.
- [78] Zhang, X., Feng, P., He, Y., Yu, T. and Sun, Q. “Experimental study on rate dependence of macroscopic domain and stress hysteresis in NiTi shape memory alloy strips”. In: *Int. J. Mech. Sci.* 52 (2010), pp. 1660–1670.
- [79] Maynadier, A., Poncelet, M., Lavernhe-Taillard, K. and Roux, S. “One-shot thermal and kinematic field measurements: Infra-Red Image Correlation”. In: *ICEM 14: 14th International Conference on Experimental Mechanics, Vol 6*. Ed. by F. Bremand. EDP Sciences, 2010, p. 38003.
- [80] Pieczyska, E. “Activity of stress-induced martensite transformation in TiNi shape memory alloy studied by infrared technique”. In: *J. Mod. Opt.* 57 (2010), pp. 1700–1707.
- [81] Vives, E., Burrows, S., Edwards, R. S., Dixon, S., Mañosa, L., Planes, A. and Romero, R. “Temperature contour maps at the strain-induced martensitic transition of a Cu-Zn-Al shape-memory single crystal”. In: *Appl. Phys. Lett.* 98 (2011), p. 011902.

- [82] Kim, K. and Daly, S. “Martensite Strain Memory in the Shape Memory Alloy Nickel-Titanium Under Mechanical Cycling”. In: *Exp. Mech.* 51 (2011), pp. 641–652.
- [83] Pieczyska, E., Dutkiewicz, J., Masdeu, F., Luckner, J. and Maciak, R. “Investigation of Thermomechanical Properties of Ferromagnetic NiFeGa Shape Memory Alloy Subjected to Pseudoelastic Compression Test”. In: *Arch. Metall. Mater.* 56 (2011), pp. 401–408.
- [84] Delpueyo, D., Balandraud, X. and Grédiac, M. “Applying infrared thermography to analyse martensitic microstructures in a Cu-Al-Be shape-memory alloy subjected to a cyclic loading”. In: *Mater. Sci. Eng. A* 528 (2011), pp. 8249–8258.
- [85] Takeda, K., Tobushi, H., Miyamoto, K. and Pieczyska, E. A. “Superelastic Deformation of TiNi Shape Memory Alloy Subjected to Various Subloop Loadings”. In: *Mater. Trans.* 53 (2012), pp. 217–223.
- [86] Pieczyska, E. A., Tobushi, H., Takeda, K. and Stró, D. “Martensite transformation bands studied in TiNi shape memory alloy by infrared and acoustic emission techniques”. In: *Kovove Mater.* 50 (2012), pp. 309–318.
- [87] Dunand-Chatellet, C. and Mounni, Z. “Coupling Infrared Thermography and Acoustic Emission Measurement to Quantify the Shakedown State of Shape Memory Alloys”. In: *Advances in Fracture and Damage Mechanics X*. Ed. by Z. Tonkovic and M. Aliabadi. Vol. 488–489. Key Engineering Materials. Trans Tech Publications Ltd, Zurich, Switzerland, 2012, pp. 146–149.
- [88] Bechtold, C., Chluba, C., De Miranda, R. and Quandt, E. “High cyclic stability of the elastocaloric effect in sputtered TiNiCu shape memory films”. In: *Appl. Phys. Lett.* 101 (2012), p. 091903.
- [89] Yan, Y., Yin, H., Sun, Q. P. and Huo, Y. “Rate dependence of temperature fields and energy dissipations in non-static pseudoelasticity”. In: *Continuum Mech. Thermodyn.* 24 (2012), pp. 675–695.
- [90] Pieczyska, E., Tobushi, H., Kulasinski, K. and Takeda, K. “Thermomechanical Coupling Effects in TiNi SMA Subjected to Compression”. In: *Mater. Trans.* 53 (2012), pp. 1905–1909.
- [91] Maynadier, A., Poncelet, M., Lavernhe-Taillard, K. and Roux, S. “One-shot Measurement of Thermal and Kinematic Fields: InfraRed Image Correlation (IRIC)”. In: *Exp. Mech.* 52 (2012), pp. 241–255.
- [92] Cui, J., Wu, Y., Muehlbauer, J., Hwang, Y., Radermacherand, R., Fackler, S., Wuttig, M. and Takeuchi, I. “Demonstration of High Efficiency Elastocaloric Cooling with Large Delta T Using NiTi Wires”. In: *Appl. Phys. Lett.* 101 (2012), p. 073904.
- [93] Reedlunn, B., Daly, S. and Shaw, J. “Superelastic shape memory alloy cables: Part I - Isothermal tension experiments”. In: *Int. J. Solids Struct.* 50 (2013), pp. 3009–3026.
- [94] Reedlunn, B., Daly, S. and Shaw, J. “Superelastic shape memory alloy cables: Part II - Sub-component isothermal responses”. In: *Int. J. Solids Struct.* 50 (2013), pp. 3027–3044.
- [95] Pieczyska, E., Tobushi, H. and Kulasinski, K. “Development of transformation bands in TiNi SMA for various stress and strain rates studied by a fast and sensitive infrared camera”. In: *Smart Mater. Struct.* 22 (2013), p. 035007.
- [96] Krevet, B., Pinneker, V., Rhode, M., Bechtold, C., Quandt, E. and Kohl, M. “Evolution of Temperature Profiles during Stress-Induced Transformation in NiTi Thin Films”. In: *European Symposium on Martensitic Transformations*. Ed. by S. Prokoshkin and N. Resnina. Vol. 738–739. Materials Science Forum. Trans Tech Publications Ltd, Zurich, Switzerland, 2013, pp. 287–292.

- [97] Ossmer, H., Chluba, C., Krevet, B., Quandt, E., Rohde, M. and Kohl, M. “Elastocaloric cooling using shape memory alloy films”. In: *13th International Conference on Micro and Nanotechnology for Power Generation and Energy Conversion Applications (POWERMEMS 2013)*. Vol. 476. Journal of Physics Conference Series. IOP Publishing Ltd, Bristol, England, 2013, p. 012138.
- [98] Du, H., Zeng, P., Zhao, J., Lei, L., Fang, G. and Qu, T. “In Situ Multi-Fields investigation on instability and transformation localization of Martensitic Phase Transformation in NiTi Alloys”. In: *Acta Metall. Sin.* 49 (2013), pp. 17–25.
- [99] Saletti, D., Pattofatto, S. and Zhao, H. “Measurement of phase transformation properties under moderate impact tensile loading in a NiTi alloy”. In: *Mech. Mater.* 65 (2013), pp. 1–11.
- [100] Cornell, S., Hartl, D. and Lagoudas, D. “Experimental Validation of a Shape Memory Alloy Constitutive Model by Heterogeneous Thermal Loading Using Infrared Thermography and Digital Image Correlation”. In: *Proceedings of the ASME Conference on Smart Materials Adaptive Structures and Intelligent Systems - 2013, Vol 2*. ASME, New York, USA, 2014, V002T02A009.
- [101] Yin, H., He, Y. and Sun, Q. “Effect of deformation frequency on temperature and stress oscillations in cyclic phase transition of NiTi shape memory alloy”. In: *J. Mech. Phys. Solids* 67 (2014), pp. 100–128.
- [102] Ossmer, H., Lambrecht, F., Gültig, M., Chluba, C., Quandt, E. and Kohl, M. “Evolution of temperature profiles in TiNi films for elastocaloric cooling”. In: *Acta Mater.* 81 (2014), pp. 9–20.
- [103] Depriester, D., Maynadier, A., Lavernhe-Taillard, K. and Hubert, O. “Thermomechanical modelling of a NiTi SMA sample submitted to displacement-controlled tensile test”. In: *Int. J. Solids Struct.* 51 (2014), pp. 1901–1922.
- [104] Ahadi, A. and Sun, Q. “Effects of grain size on the rate-dependent thermomechanical responses of nanostructured superelastic NiTi”. In: *ACTA Mater.* 76 (2014), pp. 186–197.
- [105] Pieczyska, E., Kowalczyk-Gajewska, K., Maj, M., Staszczak, M. and Tobushi, H. “Thermomechanical Investigation of TiNi Shape Memory Alloy and PU Shape Memory Polymer Subjected to Cyclic Loading”. In: *XVII International Colloquium on Mechanical Fatigue of Metals (ICMFM17)*. Ed. by M. Guagliano and L. Vergani. Vol. 74. Procedia Engineering. Elsevier Science BV, Amsterdam, Netherlands, 2014, pp. 287–292.
- [106] Daghash, S., Ozbulut, O. and Sherif, M. “Shape Memory Alloy Cables for Civil Infrastructure Systems”. In: *Proceedings of the ASME Conference on Smart Materials Adaptive Structures and Intelligent Systems, 2014, Vol 1*. ASME, New York, USA, 2014, V001T01A017.
- [107] Maletta, C., Bruno, L., Corigliano, P., Crupi, V. and Guglielmino, E. “Crack-tip thermal and mechanical hysteresis in Shape Memory Alloys under fatigue loading”. In: *Mater. Sci. Eng. A* 616 (2014), pp. 281–287.
- [108] Pelegrina, J., Yawny, A., Olbricht, J. and Eggeler, G. “Transformation activity in ultrafine grained pseudoelastic NiTi wires during small amplitude loading/unloading experiments”. In: *J. Alloys Compd.* 651 (2015), pp. 655–665.
- [109] Pieczyska, E. A. “Mechanical behavior and infrared imaging of ferromagnetic NiFeGaCo SMA single crystal subjected to subsequent compression cycles”. In: *Arch. Metall. Mater.* (2015), pp. 585–590.
- [110] Delobelle, V., Favier, D., Louche, H. and Connesson, N. “Determination of Local Thermophysical Properties and Heat of Transition from Thermal Fields Measurement During Drop Calorimetric Experiment”. In: *Exp. Mech.* 55 (2015), pp. 711–723.
- [111] Pataky, G. J., Ertekin, E. and Sehitoglu, H. “Elastocaloric cooling potential of NiTi, Ni₂FeGa, and CoNiAl”. In: *Acta Mater.* 96 (2015), pp. 420–427.

- [112] Xiao, Y., Zeng, P., Lei, L. and Du, H. “Experimental Investigation on Rate Dependence of Thermomechanical Response in Superelastic NiTi Shape Memory Alloy”. In: *J. Mater. Eng. Perform.* 24 (2015), pp. 3755–3760.
- [113] Alarcon, E., Heller, L., Chirani, S., Sittner, P., Saint-Sulpice, L. and Calloch, S. “Phase Transformations and Fatigue of NiTi”. In: *ESOMAT 2015, 10th European Symposium on Martensitic Transformations*. Ed. by N. Schryvers and J. VanHumbeeck. Vol. 33. EDP Sciences, 2015, p. 03011.
- [114] Ossmer, H., Chluba, C., Gueltig, M., Quandt, E. and Kohl, M. “Local Evolution of the Elastocaloric Effect in TiNi-Based Films”. In: *Shap. Mem. Superelasticity* 1 (2015), pp. 142–152.
- [115] Schmidt, M., Schutze, A. and Seelecke, S. “Scientific test setup for investigation of Shape memory alloy based elastocaloric cooling processes”. In: *Int. J. Refrig.* 54 (2015), pp. 88–97.
- [116] Ossmer, H., Miyazaki, S. and Kohl, M. “The Elastocaloric Effect in TiNi-based Foils”. In: *Materials Today-Proceedings*. Vol. 2. Elsevier Science BV, Amsterdam, Netherlands, 2015, pp. 971–974.
- [117] Tusek, J., Engelbrecht, K., Eriksen, D., Dall’Olio, S., Tusek, J. and Pryds, N. “A regenerative elastocaloric heat pump”. In: *Nat. Energy* 1 (2016), p. 16134.
- [118] Michalak, M. and Krucin, I. “A smart fabric with increased insulating properties”. In: *Text. Res. J.* 86 (2016), pp. 97–111.
- [119] Ozbulut, O., Daghash, S. and Sherif, M. “Shape Memory Alloy Cables for Structural Applications”. In: *J. Mater. Civ. Eng.* 28 (2016), p. 04015176.
- [120] Schmidt, M., Ullrich, J., Wiecek, A., Frenzel, J., Eggeler, G., Schütze, A. and Seelecke, S. “Experimental Methods for Investigation of Shape Memory Based Elastocaloric Cooling Processes and Model Validation”. In: *J. Vis. Exp.* 111 (2016), p. 53626.
- [121] Kan, Q., Yu, C., Kang, G., Li, J. and Yan, W. “Experimental observations on rate-dependent cyclic deformation of super-elastic NiTi shape memory alloy”. In: *Mech. Mater.* 97 (2016), pp. 48–58.
- [122] Xie, X., Kan, Q., Kang, G., Li, J., Qiu, B. and Yu, C. “Observation on the transformation domains of super-elastic NiTi shape memory alloy and their evolutions during cyclic loading”. In: *Smart Mater. Struct.* 25 (2016), p. 045003.
- [123] Bechle, N. J. and Kyriakides, S. “Evolution of phase transformation fronts and associated thermal effects in a NiTi tube under a biaxial stress state”. In: *Extrem. Mech. Lett.* 8 (2016), pp. 55–63.
- [124] Bruederlin, F., Ossmer, H., Wendler, F., Miyazaki, S. and Kohl, M. “SMA foil-based elastocaloric cooling: from material behavior to device engineering”. In: *J. Phys. D Appl. Phys.* 50 (2017), p. 424003.
- [125] Xia, M. and Sun, Q. “Thermomechanical responses of nonlinear torsional vibration with NiTi shape memory alloy - Alternative stable states and their jumps”. In: *J. Mech. Phys. Solids* 102 (2017), pp. 257–276.
- [126] Alarcon, E., Heller, L., Chirani, S. A., Sittner, P., Kopecek, J., Saint-Sulpice, L. and Calloch, S. “Fatigue performance of superelastic NiTi near stress-induced martensitic transformation”. In: *Int. J. Fatigue* 95 (2017), pp. 76–89.
- [127] You, Y., Zhang, Y., Moumni, Z., Anlas, G. and Zhang, W. “Effect of the thermomechanical coupling on fatigue crack propagation in NiTi shape memory alloys”. In: *Mater. Sci. Eng. A* 685 (2017), pp. 50–56.
- [128] Zhang, Y., You, Y., Moumni, Z., Anlas, G. and Zhu, J. “Experimental and theoretical investigation of the frequency effect on low cycle fatigue of shape memory alloys”. In: *Int. J. Plast.* 90 (2017), pp. 1–30.

- [129] Shen, A., Zhao, D., Sun, W., Liu, J. and Li, C. “Elastocaloric effect in a Co₅₀Ni₂₀Ga₃₀ single crystal”. In: *Scr. Mater.* 127 (2017), pp. 1–5.
- [130] Zhao, D., Liu, J., Chen, X., Sun, W., Li, Y., Zhang, M., Shao, Y., Zhang, H. and Yan, A. “Giant caloric effect of low-hysteresis metamagnetic shape memory alloys with exceptional cyclic functionality”. In: *Acta Mater.* 133 (2017), pp. 217–223.
- [131] Sun, W., Liu, J., Zhao, D. and Zhang, M. “Directional solidification and elastocaloric effect in a Ni₄₅Mn₄₄Sn₁₁ magnetic shape memory alloy”. In: *J. Phys. D: Appl. Phys.* 50 (2017), p. 444001.
- [132] Pieczyska, E., Kowalewski, Z. and Dunic, V. “Stress Relaxation Effects in TiNi SMA During Superelastic Deformation: Experiment and Constitutive Model”. In: *Shap. Mem. Superelasticity* 3 (2017), pp. 392–402.
- [133] Xiao, F., Chen, H., Jin, X., Nie, Z., Kakeshita, T. and Fukuda, T. “Stress-induced reverse martensitic transformation in a Ti-51Ni (at%) alloy aged under uniaxial stress”. In: *Sci. Rep.* 8 (2018), p. 6099.
- [134] Sharar, D., Radice, J., Warzoha, R., Hanrahan, B. and Chang, B. “First Demonstration of a Bending-Mode Elastocaloric Cooling ‘Loop’”. In: *Proceedings of the 17th IEEE Intersociety Conference on Thermal and Thermomechanical Phenomena in Electronic Systems (ITHERM 2018)*. IEEE, New York, USA, 2018, pp. 218–226.
- [135] Tusek, J., Zerovnik, A., Cebon, M., Brojan, M., Zuzek, B., Engelbrecht, K. and Cadelli, A. “Elastocaloric effect vs fatigue life: Exploring the durability limits of Ni-Ti plates under pre-strain conditions for elastocaloric cooling”. In: *Acta Mater.* 150 (2018), pp. 295–307.
- [136] Yan, K., Wei, P., Ren, F., He, W. and Sun, Q. “Enhance Fatigue Resistance of Nanocrystalline NiTi by Laser Shock Peening”. In: *Shap. Mem. Superelasticity* 5 (2019), pp. 436–443.
- [137] Fritsch, E., Izadi, M. and Ghafoori, E. “Development of nail-anchor strengthening system with iron-based shape memory alloy (Fe-SMA) strips”. In: *Constr. Build. Mater.* 229 (2019), p. 117042.
- [138] Shen, Y., Sun, W., Wei, Z., Shen, Q., Zhang, Y. and Liu, J. “Orientation dependent elastocaloric effect in directionally solidified Ni-Mn-Sn alloys”. In: *Scr. Mater.* 163 (2019), pp. 14–18.
- [139] Wei, Z., Sun, W., Shen, Q., Shen, Y., Zhang, Y., Liu, E. and Liu, J. “Elastocaloric effect of all-d-metal Heusler NiMnTi(Co) magnetic shape memory alloys by digital image correlation and infrared thermography”. In: *Appl. Phys. Lett.* 114 (2019), p. 101903.
- [140] Shariat, B. S., Bakhtiari, S., Yang, H. and Liu, Y. “Experimental and numerical data for transformation propagation in NiTi shape memory structures”. In: *Data in Brief* 27 (2019), p. 104566.
- [141] Michaelis, N., Welsch, F., Kirsch, S. M., Seelecke, S. and Schütze, A. “Resistance monitoring of shape memory material stabilization during elastocaloric training”. In: *Smart Mater. Struct.* 28 (2019), p. 105046.
- [142] Shariat, B. S., Bakhtiari, S., Yang, H. and Liu, Y. “Computational and experimental analyses of martensitic transformation propagation in shape memory alloys”. In: *J. Alloys Compd.* 806 (2019), pp. 1522–1528.
- [143] Kabirifar, P., Zerovnik, A., Ahcin, Z., Porenta, L., Brojan, M. and Tusek, J. “Elastocaloric Cooling: State-of-the-art and Future Challenges in Designing Regenerative Elastocaloric Devices”. In: *Strojnicki Vestnik-J. Mech. Eng.* (2019), pp. 615–630.
- [144] Sharar, D., Donovan, B., Warzoha, R., Wilson, A., Leff, A. and Hanrahan, B. “Solid-state thermal energy storage using reversible martensitic transformations”. In: *Appl. Phys. Lett.* 114 (2019), p. 143902.

- [145] You, Y., Gu, X., Zhang, Y., Moumni, Z., Anlas, G. and Zhang, W. “Effect of thermomechanical coupling on stress-induced martensitic transformation around the crack tip of edge cracked shape memory alloy”. In: *Int. J. Fracture* 216 (2019), pp. 123–133.
- [146] Jury, A., Balandraud, X., Heller, L., Alarcon, E. and Karlik, M. “One-Dimensional Heat Source Reconstruction Applied to Phase Transforming Superelastic Ni-Ti Wire”. In: *Residual Stress, Thermomechanics & Infrared Imaging and Inverse Problems, Volume 6*. Ed. by A. Baldi, S. Kramer, F. Pierron, J. Considine, S. Bossuyt and J. Hoefnagels. Conference Proceedings of the Society for Experimental Mechanics Series. Springer, Cham, Switzerland, 2020, pp. 33–40.
- [147] Shen, Y., Wei, Z., Sun, W., Zhang, Y., Liu, E. and Liu, J. “Large elastocaloric effect in directionally solidified all-d-metal Heusler metamagnetic shape memory alloys”. In: *Acta Mater.* 188 (2020), pp. 677–685.
- [148] Asfaw, A., Sherif, M., Xing, G. and Ozbulut, O. “Experimental Investigation on Buckling and Post-buckling Behavior of Superelastic Shape Memory Alloy Bars”. In: *J. Mater. Eng. Perform.* 29 (2020), pp. 3127–3140.
- [149] Wang, J., Ren, X., Xu, Y., Zhang, W., Zhu, J. and Li, B. “Thermodynamic behavior of NiTi shape memory alloy against low-velocity impact: experiment and simulation”. In: *Int. J. Impact Eng.* 139 (2020), p. 103532.
- [150] Furgiele, F., Magarò, P., Maletta, C. and Sgambitterra, E. “Functional and Structural Fatigue of Pseudoelastic NiTi: Global vs Local Thermo-Mechanical Response”. In: *Shape Mem. Superelasticity* 6 (2020), pp. 242–255.
- [151] Masoudi Moghaddam, S. A., Yarmohammad Tooski, M., Jabbari, M. and Khorshidvand, A. R. “Experimental investigation of sandwich panels with hybrid composite face sheets and embedded shape memory alloy wires under low velocity impact”. In: *Polym. Compos.* 41 (2020), pp. 4811–4829.
- [152] Yuan, B., Qian, M., Zhang, X. and L.Geng. “Grain structure related inhomogeneous elastocaloric effects in Cu-Al-Mn shape memory microwires”. In: *Scr. Mater.* 178 (2020), pp. 356–360.
- [153] Mutlu, F., Anlaş, G. and Moumni, Z. “Effect of loading rate on fracture mechanics of NiTi SMA”. In: *Int. J. Fracture* 224 (2020), pp. 151–165.
- [154] Ianniciello, L., Romanini, M., Manosa, L., Planes, A., Engelbrecht, K. and Vives, E. “Tracking the dynamics of power sources and sinks during the martensitic transformation of a Cu-Al-Ni single crystal”. In: *Appl. Phys. Lett.* 116 (2020), p. 183901.
- [155] Nataf, G., Romanini, M., Vives, E., Zuzek, B., Planes, A., Tusek, J. and Moya, X. “Suppression of acoustic emission during superelastic tensile cycling of polycrystalline Ni_{50.4}Ti_{49.6}”. In: *Phys. Rev. Mater.* 4 (2020), p. 093604.
- [156] Li, M., Chen, M. and Sun, Q. “Nonlocal modeling and analysis of spatiotemporal patterns in non-isothermal phase transformation of NiTi strips”. In: *Int. J. Solids Struct.* 221 (2021), pp. 103–116.
- [157] Shariat, B. S., Bakhtiari, S., Yang, H. and Liu, Y. “Controlled initiation and propagation of stress-induced martensitic transformation in functionally graded NiTi”. In: *J. Alloys Compd.* 851 (2021), p. 156103.
- [158] Alarcon, E. and Heller, L. “Deformation infrared calorimetry for materials characterization applied to study cyclic superelasticity in NiTi wires”. In: *Mater. Des.* 199 (2021), p. 109406.
- [159] Kilic, U., Daghash, S., Sherif, M. and Ozbulut, O. “Tensile characterization of graphene nanoplatelet/shape memory alloy/epoxy composites using digital and thermal imaging”. In: *Polym. Compos.* 42 (2021), pp. 1235–1244.

- [160] Jongchansitto, P., Yachai, T., Preechawuttipong, I., Boufayed, R. and Balandraud, X. “Concept of mechanocaloric granular material made from shape memory alloy”. In: *Energy* 219 (2021), p. 119656.
- [161] Lu, N. and Chen, C. “Inhomogeneous martensitic transformation behavior and elastocaloric effect in a bicrystal Cu-Al-Mn shape memory alloy”. In: *Mater. Sci. Eng. A* 800 (2021), p. 140386.
- [162] Sharar, D., Radice, J., Warzoha, R., Hanrahan, B. and Smith, A. “Low-force elastocaloric refrigeration via bending”. In: *Appl. Phys. Lett.* 118 (2021), p. 184103.
- [163] Shastry, V., Singh, G. and Ramamurty, U. “On the fatigue life enhancement due to periodic healing of a NiTi shape memory alloy”. In: *Mater. Sci. Eng. A* (2021), p. 141272.
- [164] Calloch, S., Bouvet, C., Hild, F., Doudard, C. and LExcellent, C. “Analysis of mechanical behavior and in-situ observations of Cu-Al-Be SMA under biaxial compressive tests by using DIC”. In: *Third International Conference on Experimental Mechanics*. Ed. by X. Wu, Y. Qin, J. Fang and J. Ke. Vol. 4537. Proceedings of the Society of Photo-Optical Instrumentation Engineers (SPIE). 2002, pp. 83–86.
- [165] Moore, C. L. and Bruck, H. A. “A fundamental investigation into large strain recovery of one-way shape memory alloy wires embedded in flexible polyurethanes”. In: *Smart Mater. Struct.* 11 (2002), pp. 130–139.
- [166] Bruck, H. A., Moore, C. L. and Valentine, T. L. “Repeatable bending actuation in polyurethanes using opposing embedded one-way shape memory alloy wires exhibiting large deformation recovery”. In: *Smart Mater. Struct.* 11 (2002), p. 305.
- [167] Umezaki, E. and Ichikawa, T. “Measurement of Deformation of Epoxy Resin Plates with an Embedded SMA Wire Using Digital Image Correlation”. In: *Int. J. Mod. Phys. B* 17 (2003), pp. 1750–1755.
- [168] Bruck, H. A., Moore, C. L. and Valentine, T. M. “Bending Actuation in Polyurethanes with a Symmetrically Graded Distribution of One-way Shape Memory Alloy Wires”. In: *Exp. Mech.* 44 (2004).
- [169] Murasawa, G., Yoneyama, S., Sakuma, T. and Takashi, M. “Influence of Cyclic Loading on Inhomogeneous Deformation Behavior Arising in NiTi Shape Memory Alloy Plate”. In: *Mater. Trans.* 47 (2006), pp. 780–786.
- [170] Murasawa, G. and Yoneyama, S. “Local Strain Distribution Arising in Shape Memory Alloy Composite Subjected to Thermal Loading”. In: *Mater. Trans.* 47 (2006), pp. 766–771.
- [171] Shen, L., He, J., Su, Y., Chu, W. and Qiao, L. “In situ study of cracking for Ni₂MnGa ferromagnetic shape memory alloy”. In: *Acta Metall. Sin.* 42 (2006), pp. 810–814.
- [172] Dutta, I., Pan, D., Ma, S., Majumdar, B. and S. Harris, S. “Role of Shape-memory Alloy Reinforcements on Strain Evolution in Lead-free Solder Joints”. In: *Electron. Mater.* 35 (2006), pp. 1902–1913.
- [173] Murasawa, G., Yoneyama, S. and Sakuma, T. “Nucleation, bifurcation and propagation of local deformation arising in NiTi shape memory alloy”. In: *Smart Mater. Struct.* 16 (2007), pp. 160–167.
- [174] Daly, S., Ravichandran, G. and Bhattacharya, K. “Stress-induced martensitic phase transformation in thin sheets of Nitinol”. In: *Acta Mater.* 55 (2007), pp. 3593–3600.
- [175] Daly, S., Miller, A., Ravichandran, G. and Bhattacharya, K. “An experimental investigation of crack initiation in thin sheets of nitinol”. In: *Acta Mater.* 55 (2007), pp. 6322–6330.
- [176] Hamilton, R., Sehitoglu, H., Aslantas, K., Efstathiou, C. and Maier, H. “Intermartensite strain evolution in NiMnGa single crystals”. In: *Acta Mater.* 56 (2008), pp. 2231–2236.

- [177] Efstathiou, C., Sehitoglu, H., Carroll, J., Lambros, J. and Maier, H. J. “Full-field strain evolution during intermartensitic transformations in single-crystal NiFeGa”. In: *Acta Mater.* 56 (2008), pp. 3791–3799.
- [178] Sánchez-Arévalo, F. M. and Pulos, G. “Use of digital image correlation to determine the mechanical behavior of materials”. In: *Mater. Charact.* 59 (2008), pp. 1572–1579.
- [179] Efstathiou, C. and Sehitoglu, H. “Local transformation strain measurements in precipitated NiTi single crystals”. In: *Scr. Mater.* 59 (2008), pp. 1263–1266.
- [180] Daly, S., Rittel, D., Bhattacharya, K. and Ravichandran, G. “Large Deformation of Nitinol Under Shear Dominant Loading”. In: *Exp. Mech.* 49 (2009), pp. 225–233.
- [181] Merzouki, T., Collard, C., Bourgeois, N., Zineb, T. and Meraghni, F. “Coupling between experiment and numerical simulation of shape memory alloy multicrystal”. In: *ESOMAT 2009 - 8th European Symposium on Martensitic transformations*. Ed. by P. Sittner, V. Paidar, L. Heller and H. Seiner. EDP Sciences, 2009, p. 06035.
- [182] Daly, S., Rittel, D., Bhattacharya, K. and Ravichandran, G. “Large Deformation of Nitinol Under Shear Dominant Loading”. In: *Exp. Mech.* 49 (2009), pp. 225–233.
- [183] Murasawa, G., Kitamura, K., Yoneyama, S., Miyazaki, S., Miyata, K., Nishioka, A. and Koda, T. “Macroscopic stress-strain curve, local strain band behavior and the texture of NiTi thin sheets”. In: *Smart Mater. Struct.* 18 (2009), p. 055003.
- [184] Sánchez-Arévalo, F., Garcia-Fernández, T., Pulos, G. and Villagrán-Muniz, M. “Use of digital speckle pattern correlation for strain measurements in a CuAlBe shape memory alloy”. In: *Mater. Charact.* 60 (2009), pp. 775–782.
- [185] Schaefer, A. and Wagner, M. “Strain mapping at propagating interfaces in pseudoelastic NiTi”. In: *ESOMAT 2009 - 8th European Symposium on Martensitic Transformations*. Ed. by P. Sittner, V. Paidar, L. Heller and H. Seiner. EDP Sciences, 2009, p. 06031.
- [186] Bourgeois, N., Meraghni, F. and Ben Zineb, T. “Measurement of local strain heterogeneities in superelastic shape memory alloys by digital image correlation”. In: *3rd International Symposium on Shape Memory Materials for Smart Systems/E-MRS Spring Meeting*. Ed. by M. Kohl and V. Chernenko. Vol. 10. Physics Procedia. Elsevier Science BV, Amsterdam Netherlands, 2010, pp. 4–10.
- [187] Lackmann, J., Regenspurger, R., Maxisch, M., Grundmeier, G. and Maier, H. J. “Defect formation in thin polyelectrolyte films on polycrystalline NiTi substrates”. In: *J. Mech. Behav. Biomed. Mater.* 3 (2010), pp. 436–445.
- [188] Dadda, J., Maier, H., Karaman, I. and Chumlyakov, Y. “High-temperature in-situ microscopy during stress-induced phase transformations in Co₄₉Ni₂₁Ga₃₀ shape memory alloy single crystals”. In: *Int. J. Mater. Res.* 101 (2010), pp. 1503–1513.
- [189] Merzouki, T., Collard, C., Bourgeois, N., Zineb, T. B. and Meraghni, F. “Coupling between measured kinematic fields and multicrystal SMA finite element calculations”. In: *Mech. Mater.* 42 (2010), pp. 72–95.
- [190] Dilibal, S., Sehitoglu, H., Hamilton, R. F., Maier, H. J. and Chumlyakov, Y. “On the volume change in Co-Ni-Al during pseudoelasticity”. In: *Mater. Sci. Eng. A* 528 (2010), pp. 2875–2881.
- [191] Murasawa, G., Yoneyama, S., Miyata, K., Nishioka, A. and Koda, T. “Finite element analysis and experimental measurement of deformation behavior for NiTi plate with stress concentration part under uniaxial tensile loading”. In: *Strain* 47 (2011), pp. 389–397.
- [192] Hamilton, R. F., Dilibal, S., Sehitoglu, H. and Maier, H. J. “Underlying mechanism of dual hysteresis in NiMnGa single crystals”. In: *Mater. Sci. Eng. A* 528 (2011), pp. 1877–1881.
- [193] Lackmann, J., Niendorf, T., Maxisch, M., Grundmeier, G. and Maier, H. J. “High-resolution in-situ characterization of the surface evolution of a polycrystalline NiTi SMA-alloy under pseudoelastic deformation”. In: *Mater. Charact.* 42 (2011), pp. 298–303.

- [194] Grolleau, V., Louche, H., Delobelle, V., Penin, A., Rio, G., Liu, Y. and Favier, D. “Assessment of tension-compression asymmetry of NiTi using circular bulge testing of thin plates”. In: *Scr. Mater.* 65 (2011), pp. 347–350.
- [195] Reedlunn, B., Churchill, C., Nelson, E., Daly, S. and Shaw, J. “Bending of Superelastic Shape Memory Alloy Tubes”. In: *Proceedings of the ASME Conference on Smart Materials Adaptive Structures and Intelligent Systems (SMASIS 2011), Vol 1*. ASME, New York, USA, 2012, pp. 249–258.
- [196] Reedlunn, B., Daly, S. and Shaw, J. “Tension-Torsion Experiments on Superelastic Shape Memory Alloy Tubes”. In: *Proceedings of the ASME Conference on Smart Materials Adaptive Structures and Intelligent Systems, Vol 2*. ASME, New York, USA, 2012, pp. 213–222.
- [197] Taillebot, V., Lexcellent, C. and Vacher, P. “About the transformation phases zones of shape memory alloys’ fracture tests on single-edge-cracked specimen.” In: *Funct. Mater. Lett.* 05 (2012), p. 1250007.
- [198] Zeng, P., Du, H., Zhao, J., Lei, L., Sun, G. F. C. and Gao, Y. “Advances on experiment, measure and numerical simulation for behaviors of material processes”. In: *11th International Conference on Numerical Methods in Industrial Forming Processes (NUMIFORM 2013)*. Ed. by S. Zhang, X. Liu and M. Cheng. Vol. 1532. AIP Conference Proceedings. Ameri. Inst. Physics, Melville, USA, 2013, pp. 38–44.
- [199] Chemisky, Y., Echchorfi, R., Meraghni, F., Bourgeois, N. and Piotrowski, B. “Determination of the characteristic parameters of tension-compression asymmetry of Shape Memory Alloys using full-field measurements”. In: *European Symposium on Martensitic Transformations*. Ed. by S. Prokoshkin and N. Resnina. Vol. 738–739. Materials Science Forum. Trans Tech Publications Ltd, Zurich, Switzerland, 2013, p. 281.
- [200] Bewerse, C., Gall, K. R., Mcfarland, G. J., Zhu, P. and Brinson, L. C. “Local and global strains and strain ratios in shape memory alloys using digital image correlation”. In: *Mater. Sci. Eng. A* 568 (2013), pp. 134–142.
- [201] Bubulinca, C., Balandraud, X., Delpueyo, D., Grédiac, M., Stanciu, S., Abrudeanu, M., Plaiasu, A. G., Dicu, M. M. and Nitu, E. L. “Study of a monocrystalline Cu-Al-Ni shape memory alloy by infrared thermography”. In: *J. Optoelectron. Adv. Mater.* 15 (2013), pp. 544–549.
- [202] He, H., Saletti, D., Pattofatto, S., Shi, F. and Zhao, H. “Experimental observation of phase transformation front of SMA under impact loading”. In: *13th International Conference on Fracture 2013 (ICF-13)*. Ed. by S. Prokoshkin and N. Resnina. Vol. 4. International Congress on Fracture (ICF), 2013, pp. 2658–2666.
- [203] Chen, X., He, Y. and Moumni, Z. “Twin boundary motion in NiMnGa single crystals under biaxial compression”. In: *Mater. Lett.* 90 (2013), pp. 72–75.
- [204] Kim, K. and Daly, S. “The Effect of Texture on Stress-Induced Martensite Formation in Nickel-Titanium”. In: *Smart Mater. Struct.* 22 (2013), p. 075012.
- [205] Watkins, R., Reedlunn, B. and Shaw, J. “Uniaxial, Pure Bending and Buckling Characterization of Superelastic NiTi Rods and Tubes: An Experimental Study”. In: *Proceedings of the ASME Conference on Smart Materials Adaptive Structures and Intelligent Systems, 2014, Vol 2*. ASME, New York, USA, 2014, V002T02A003.
- [206] Cornell, S., Leser, W., Hochhalter, J., Newman, J. and Hartl, J. “Development and Characterization of Embedded Sensory Particles using Multi-Scale 3D Digital Image Correlation”. In: *Proceedings of the ASME Conference on Smart Materials Adaptive Structures and Intelligent Systems, 2014, Vol 2*. ASME, New York, USA, 2014, V002T02A010.
- [207] Pinneker, V., Gueltig, M., Sozinov, A. and Kohl, M. “Single phase boundary actuation of a ferromagnetic shape memory foil”. In: *Acta Mater.* 64 (2014), pp. 179–187.

- [208] Bechle, N. and Kyriakides, S. “Localization in NiTi tubes under bending”. In: *Int. J. Solids Struct.* 51 (2014), pp. 967–980.
- [209] Shafaghi, N., Haghgouyan, B., Aydiner, C. C. and Anlas, G. “Experimental and computational evaluation of crack-tip displacement field and transformation zone in NiTi”. In: *Mater. Today Proc.* 2 (2015), S763–S766.
- [210] Sgambitterra, E., Lesci, S. and Maletta, C. “Effects of Higher Order Terms in Fracture Mechanics of Shape Memory Alloys by Digital Image Correlation”. In: *XXIII Italian Group of Fracture Meeting, IGFXIII*. Ed. by F. Iacoviello, G. Ferro and L. Susmel. Vol. 109. Procedia Engineering. Elsevier Science BV, Amsterdam, Netherlands, 2015, pp. 457–464.
- [211] Chemisky, Y., Meraghni, F., Bourgeois, N., Cornell, S., Echchorfi, R. and Patoor, E. “Identification of Model Parameter for the Simulation of SMA Structures Using Full Field Measurements”. In: *Proceedings of the TMS Middle East - Mediterranean Materials Congress on Energy and Infrastructure Systems (MEMA 2015)*. Ed. by I. Karaman, R. Arroyave and E. Masad. Wiley-Blackwell, Malden, USA, 2015, pp. 191–200.
- [212] Chemisky, Y., Meraghni, F., Bourgeois, N., Cornell, S., Echchorfi, R. and Patoor, E. “Analysis of the deformation paths and thermomechanical parameter identification of a shape memory alloy using digital image correlation over heterogeneous tests”. In: *Int. J. Mech. Sci.* 96–97 (2015), pp. 13–24.
- [213] Elibol, C. and Wagner, M. F. X. “Investigation of the stress-induced martensitic transformation in pseudoelastic NiTi under uniaxial tension, compression and compression-shear”. In: *Mater. Sci. Eng. A* 621 (2015), pp. 76–81.
- [214] Patriarca, L. and Sehitoglu, H. “High-temperature superelasticity of Ni_{50.6}Ti_{24.4}Hf_{25.0} shape memory alloy”. In: *Scr. Mater.* 101 (2015), pp. 12–15.
- [215] El-Tahan, M., Dawood, M. and Song, G. “Development of a self-stressing NiTiNb shape memory alloy (SMA)/fiber reinforced polymer (FRP) patch”. In: *Smart Mater. Struct.* 24 (2015), p. 065035.
- [216] Lanba, A. and Hamilton, R. F. “The Impact of Martensite Deformation on Shape Memory Effect Recovery Strain Evolution”. In: *Metall. Mater. Trans. A* 46 (2015), pp. 3481–3489.
- [217] Kimiecik, M., Jones, J. W. and Daly, S. “Grain orientation dependence of phase transformation in the shape memory alloy Nickel-Titanium”. In: *Acta Mater.* 94 (2015), pp. 214–223.
- [218] Laydi, M. and LExcellent, C. “Phase Transformation Surfaces Analysis for SMA Around a Crack Tip with Curvature”. In: *Shap. Mem. Superelasticity* 1 (2015), pp. 339–346.
- [219] Ojha, A., Alkan, S., Patriarca, L., Sehitoglu, H. and Chumlyakov, Y. “Shape memory behavior in Fe₃Al-modeling and experiments”. In: *Philos. Mag.* (2015).
- [220] Ojha, A., Patriarca, L. and Sehitoglu, H. “Pseudoelasticity in Fe₃Ga with boron-A combined atomistic-micromechanical treatment”. In: *Int. J. Plasticity* 72 (2015), pp. 185–199.
- [221] Elibol, C. and Wagner, X. “Strain rate effects on the localization of the stress-induced martensitic transformation in pseudoelastic NiTi under uniaxial tension, compression and compression-shear”. In: *Mater. Sci. Eng. A* 643 (2015), pp. 194–202.
- [222] Kimiecik, M., Jones, J. and Daly, S. “Grain orientation dependence of phase transformation in the shape memory alloy Nickel-Titanium”. In: *Acta Mater.* 94 (2015), pp. 214–223.
- [223] Wu, Y., Patriarca, L., Li, G., Sehitoglu, H., Soejima, Y., Ito, T. and Nishida, M. “Shape Memory Response of Polycrystalline NiTi_{12.5}Hf Alloy: Transformation at Small Scales”. In: *Shap. Mem. Superelasticity* 1 (2015), pp. 387–397.
- [224] Sgambitterra, E., Maletta, C. and Furguele, F. “Investigation on Crack Tip Transformation in NiTi Alloys: Effect of the Temperature”. In: *Shap. Mem. Superelasticity* 1 (2015), pp. 275–283.

- [225] Xiao, Y., Zeng, P. and Lei, L. “Experimental Investigation on the Mechanical Instability of Superelastic NiTi Shape Memory Alloy”. In: *J. Mater. Eng. Perform.* 25 (2016), pp. 3551–3557.
- [226] Ossmer, H., Chluba, C., Quandt, E. and Kohl, M. “TiNi-based films for elastocaloric microcooling-Fatigue life and device performance.” In: *APL Mater.* 064102 (2016).
- [227] Xiao, Y., Zeng, P. and Lei, L. “Experimental investigation on local mechanical response of superelastic NiTi shape memory alloy”. In: *Smart Mater. Struct.* 25 (2016).
- [228] Patriarca, L., Sehitoglu, H., Panchenko, E. and Chumlyakov, Y. “High-temperature functional behavior of single crystal Ni_{51.2}Ti_{23.4}Hf_{25.4} shape memory alloy”. In: *Acta Mater.* 106 (2016), pp. 333–343.
- [229] Kimiecik, M., Jones, J. W. and Daly, S. “The effect of microstructure on stress-induced martensitic transformation under cyclic loading in the SMA Nickel-Titanium”. In: *J. Mech. Phys. Solids* 89 (2016), pp. 16–30.
- [230] Patriarca, L., Wu, Y., Sehitoglu, H. and Chumlyakov, Y. “High temperature shape memory behavior of Ni_{50.3}Ti₂₅Hf_{24.7} single crystals”. In: *Scr. Mater.* 115 (2016), pp. 133–136.
- [231] Wu, Y., Patriarca, L., Sehitoglu, H. and Chumlyakov, Y. “Ultrahigh tensile transformation strains in new Ni_{50.5}Ti_{36.2}Hf_{13.3} shape memory alloy”. In: *Scr. Mater.* 118 (2016), pp. 51–54.
- [232] Haghgouyan, B., Shafaghi, N., Aydmer, C. and Anlas, G. “Experimental and computational investigation of the effect of phase transformation on fracture parameters of an SMA”. In: *Smart Mater. Struct.* 25 (2016), p. 075010.
- [233] LePage, W. S., Daly, S. H. and Shaw, J. A. “Cross Polarization for Improved Digital Image Correlation”. In: *Exp. Mech.* 56 (2016), pp. 969–985.
- [234] Bimber, B. A., Hamilton, R. F., Keist, J. and Palmer, T. A. “Anisotropic microstructure and superelasticity of additive manufactured NiTi alloy bulk builds using laser directed energy deposition”. In: *Mater. Sci. Eng. A* 674 (2016), pp. 125–134.
- [235] Xiao, Y., Zeng, P. and Lei, L. “Experimental observations on mechanical response of three-phase NiTi shape memory alloy under uniaxial tension”. In: *Mater. Res. Express* 3 (2016), p. 105701.
- [236] Xiao, Y., Zeng, P. and Lei, L. “Effect of double-edge semi-circular notches on the mechanical response of superelastic NiTi shape memory alloy: Experimental observations”. In: *J. Strain Anal. Eng. Des.* 51 (2016), pp. 555–562.
- [237] Murasawa, G., Yeduru, S. R. and Kohl, M. “Macroscopic inhomogeneous deformation behavior arising in single crystal Ni-Mn-Ga foils under tensile loading”. In: *Opt. Lasers Eng.* 87 (2016), pp. 139–145.
- [238] Gong, J. and Daly, S. “Microscale Repeatability of the Shape-Memory Effect in Fine NiTi Wires”. In: *Shap. Mem. Superelasticity* 2 (2016), pp. 298–309.
- [239] Maletta, C., Sgambitterra, E. and Niccoli, F. “Temperature dependent fracture properties of shape memory alloys: novel findings and a comprehensive model”. In: *Sci. Rep.* 6 (2016), p. 17.
- [240] Wheeler, R., Ottmers, C., Hewling, B. and Lagoudas, D. “Actuator lifetime predictions for Ni₆₀Ti₄₀ shape memory alloy plate actuators”. In: *Behavior and Mechanics of Multifunctional Materials and Composites 2016*. Ed. by N. Goulbourne. Vol. 9800. Proceedings of SPIE. SPIE-Int. Soc. Optical Engineering, Bellingham, USA, 2016, 98000E.
- [241] Xie, X., Kan, Q., Kang, G., Lu, F. and Chen, K. “Observation on rate-dependent cyclic transformation domain of super-elastic NiTi shape memory alloy”. In: *Mater. Sci. Eng. A* 671 (2016), pp. 32–47.
- [242] Sehitoglu, H., Wu, Y., Alkan, S. and Ertekin, E. “Plastic deformation of B2-NiTi - is it slip or twinning?” In: *Philos. Mag. Lett.* (2017).

- [243] Niccoli, F., Garion, C., Maletta, C., Sgambitterra, E., Furgiuele, F. and Chiggiato, P. “Beam-pipe coupling in particle accelerators by shape memory alloy rings”. In: *Mater. Des.* 114 (2017), pp. 603–611.
- [244] Xiao, Y., Zeng, P. and Lei, L. “Grain size effect on mechanical performance of nanostructured superelastic NiTi alloy”. In: *Mater. Res. Express* 4 (2017), p. 035702.
- [245] Sehitoglu, H., Wu, Y. and Patriarca, L. “Shape memory functionality under multi-cycles in NiTiHf”. In: *Scr. Mater.* 129 (2017), pp. 11–15.
- [246] Laplanche, G., Birk, T., Schneider, S., Frenzel, J. and Eggeler, G. “Effect of temperature and texture on the reorientation of martensite variants in NiTi shape memory alloys”. In: *Acta Mater.* 127 (2017), pp. 143–152.
- [247] Abuzaid, W. and Sehitoglu, H. “Functional fatigue of Ni_{50.3}Ti₂₅Hf_{24.7}. Heterogeneities and evolution of local transformation strains”. In: *Mater. Sci. Eng. A* 696 (2017), pp. 482–492.
- [248] Jiang, D., Kyriakides, S., Bechle, N. J. and Landis, C. M. “Bending of pseudoelastic NiTi tubes”. In: *Int. J. Solids Struct.* 124 (2017), pp. 192–214.
- [249] Zheng, B. and Dawood, M. “Fatigue Strengthening of Metallic Structures with a Thermally Activated Shape Memory Alloy Fiber-Reinforced Polymer Patch”. In: *J. Compos. Constr.* 21 (2017), p. 04016113.
- [250] Paul, P. P., Paranjape, H. M., Amin-Ahmadi, B., Stebner, A. P., Dunand, D. C. and Brinson, L. C. “Effect of machined feature size relative to the microstructural size on the superelastic performance in polycrystalline NiTi shape memory alloys”. In: *Mater. Sci. Eng. A* 706 (2017), pp. 227–235.
- [251] Xiao, Y., Zeng, P., Lei, L. and Zhang, Y. “In situ observation on temperature dependence of martensitic transformation and plastic deformation in superelastic NiTi shape memory alloy”. In: *Mater. Des.* 134 (2017), pp. 111–120.
- [252] Zheng, L., He, Y. and Moumni, Z. “Investigation on fatigue behaviors of NiTi polycrystalline strips under stress-controlled tension via in-situ macro-band observation”. In: *Int. J. Plast.* 90 (2017), pp. 116–145.
- [253] Shayanfard, P., Heller, L., Dostalova, D., Alarcon, E., Frost, M., Sedlak, P., Sandera, P., Sittner, P., Pokluda, J. and Hornikova, J. “Effect of martensitic transformation on local stresses and strains at a notch of cyclically loaded superelastic NiTi ribbon”. In: *14th International Conference on Fracture 2017 (ICF-14), June 18-23, 2017, Rhodes, Greece*. Ed. by E. Gdoutos. 2017.
- [254] Zotov, N., Pfund, M., Polatidis, E., Mark, A. and Mittemeijer, E. “Change of transformation mechanism during pseudoelastic cycling of NiTi shape memory alloys”. In: *Mater. Sci. Eng. A* 682 (2017), pp. 178–191.
- [255] Paranjape, H., Paul, P., Amin-Ahmadi, B., Sharma, H., Dale, D., Ko, J., Chumlyakov, Y., Brinson, L. and Stebner, A. “In situ, 3D characterization of the deformation mechanics of a superelastic NiTi shape memory alloy single crystal under multiscale constraint”. In: *Acta Mater.* 144 (2018), pp. 748–757.
- [256] Alkan, S., Wu, Y. and Sehitoglu, H. “Giant non-Schmid effect in NiTi”. In: *Extreme Mech. Lett.* 15 (2017), pp. 38–43.
- [257] Dilibal, S., Hamilton, R. and Lanba, A. “The effect of employed loading mode on the mechanical cyclic stabilization of NiTi shape memory alloys”. In: *Intermetallics* 89 (2017), pp. 1–9.
- [258] Bielefeldt, B., Hochhalter, J. and Hartl, D. “Shape memory alloy sensory particles for damage detection: Experiments, analysis, and design studies”. In: *Struct. Health Monit.* 17 (2018), pp. 777–814.

- [259] Bian, X., Saleh, A., Pereloma, E., Davies, C. and Gazder, A. “A digital image correlation study of a NiTi alloy subjected to monotonic uniaxial and cyclic loading-unloading in tension”. In: *Mater. Sci. Eng. A* 726 (2018), pp. 102–112.
- [260] Sittner, P., Sedlak, P., Seiner, H., Sedmak, P., Pilch, J., Delville, R., Heller, L. and Kaderavek, L. “On the coupling between martensitic transformation and plasticity in NiTi: Experiments and continuum based modelling”. In: *Prog. Mater. Sci.* 98 (2018), pp. 249–298.
- [261] Zhang, S. and He, Y. “Fatigue Resistance of Branching Phase-transformation Fronts in Pseudoelastic NiTi Polycrystalline Strips”. In: *Int. J. Solids Struct.* 135 (2018), pp. 233–244.
- [262] Chen, D., Sun, S., Dulieu-Barton, J., Li, Q. and Wang, W. “Crack growth analysis in welded and non-welded T-joints based on lock-in digital image correlation and thermoelastic stress analysis”. In: *Int. J. Fatigue* 110 (2018), pp. 172–185.
- [263] Hsu, W., Polatidis, E., Smid, M., Casati, N., Van Petegem, S. and Van Swygenhoven, H. “Load path change on superelastic NiTi alloys: In situ synchrotron XRD and SEM DIC”. In: *Acta Mater.* 144 (2018), pp. 874–883.
- [264] LePage, W., Ahadi, A., Lenthe, W., Sun, Q., Pollock, T., Shaw, J. and Daly, S. “Grain size effects on NiTi shape memory alloy fatigue crack growth”. In: *J. Mater. Res.* 33 (2018), pp. 91–107.
- [265] Zhang, S., Chen, X., Moumni, Z. and He, Y. “Thermal effects on high-frequency magnetic-field-induced martensite reorientation in ferromagnetic shape memory alloys: An experimental and theoretical investigation”. In: *Int. J. Plasticity* 108 (2018), pp. 1–20.
- [266] Zhang, S., Chen, X., Moumni, Z. and He, Y. “Coexistence and compatibility of martensite reorientation and phase transformation in high-frequency magnetic-field-induced deformation of Ni-Mn-Ga single crystal”. In: *Int. J. Plasticity* 110 (2018), pp. 110–122.
- [267] Bian, X., Gazder, A., Saleh, A. and Pereloma, E. “A comparative study of a NiTi alloy subjected to uniaxial monotonic and cyclic loading-unloading in tension using digital image correlation: The grain size effect”. In: *J. Alloys Compd.* 777 (2018), pp. 723–735.
- [268] Elibol, C. and Wagner, M. “Virtual Extensometer Analysis of Martensite Band Nucleation, Growth, and Strain Softening in Pseudoelastic NiTi Subjected to Different Load Cases”. In: *Materials* (2018), p. 1458.
- [269] Sgambitterra, E., Maletta, C., Furgiuele, F. and Sehitoglu, H. “Fatigue crack propagation in [012] NiTi single crystal alloy”. In: *Int. J. Fatigue* 112 (2018), pp. 9–20.
- [270] Bucsek, A., Dale, D., Ko, J., Chumlyakov, Y. and Stebner, A. “Measuring stress-induced martensite microstructures using far-field high-energy diffraction microscopy”. In: *Acta Crystallogr. A* 74 (2018), pp. 425–446.
- [271] Bucsek, A., Pagan, D., Casalena, L., Chumlyakov, Y., Mills, M. and Stebner, A. “Ferroelastic twin reorientation mechanisms in shape memory alloys elucidated with 3D X-ray microscopy”. In: *J. Mech. Phys. Solids* 124 (2019), pp. 897–928.
- [272] Chen, Y., Tyc, O., Kaderavek, L., Molnarova, O., Heller, L. and Sittner, P. “Temperature and microstructure dependence of localized tensile deformation of superelastic NiTi wires”. In: *Mater. Des.* 174 (2019), p. 107797.
- [273] Kazinakis, K., Kyriakides, S., Jiang, D., Bechle, N. and Landis, C. “Buckling and Collapse of Pseudoelastic NiTi Tubes Under Bending”. In: *Int. J. Solids Struct.* 221 (2021), pp. 2–17.
- [274] Heller, L., Šittner, P., Sedlák, P., Seiner, H., Tyc, O., Kadeřávek, L., Sedmák, P. and Vronka, M. “Beyond the strain recoverability of martensitic transformation in NiTi”. In: *Int. J. Plast.* 116 (2019), pp. 232–264.
- [275] Shuai, J. and Xiao, Y. “In-Situ Study on Texture-Dependent Martensitic Transformation and Cyclic Irreversibility of Superelastic NiTi Shape Memory Alloy”. In: *Metall. Mater. Trans. A* 51 (2019), pp. 562–567.

- [276] Wu, Y., Yaacoub, J., Brenne, F., Abuzaid, W., Canadinc, D. and Sehitoglu, H. “Deshielding Effects on Fatigue Crack Growth in Shape Memory Alloys- A study on CuZnAl single-crystalline materials”. In: *Acta Mater.* 176 (2019), pp. 155–166.
- [277] Catoor, D., Ma, Z. and Kumar, S. “Cyclic response and fatigue failure of Nitinol under tension loading”. In: *J. Mater. Res.* 34 (2019), pp. 3504–3522.
- [278] Bahador, A., Umeda, J., Tsutsumi, S., Hamzah, E., Yusof, F., Fujii, H. and Kondoh, K. “Asymmetric local strain, microstructure and superelasticity of friction stir welded Nitinol alloy”. In: *Mater. Sci. Eng. A* 767 (2019), p. 138344.
- [279] Kumar, S., Marandi, L., Balla, V., Bysakh, S., Piorunek, D., Eggeler, G., Das, M. and Sen, I. “Microstructure - Property correlations for additively manufactured NiTi based shape memory alloys”. In: *Materialia* 8 (2019), p. 100456.
- [280] Kyianytsia, A., Ponçot, M., Letoffe, A., Boulet, P., Migot, S., Ghanbaja, J., Cinar, I., de Miranda, R., Bechtold, C., Kierren, B., Ozatay, O. and Hauet, T. “Magnetic anisotropy switching induced by shape memory effect in NiTi/Ni bilayer”. In: *Appl. Phys. Lett.* 115 (2019), p. 222402.
- [281] Ma, L., Li, Y. and Han, G. “Study on fracture behavior of NiTi Alloy by the digital image correlation method”. In: *7th Global Conference on Materials Science and Engineering (CMSE2018)*. Ed. by A. Khotsianovsky. Vol. 474. IOP Conference Series- Materials Science and Engineering. IOP Publishing Ltd, Bristol, England, 2019, p. 012053.
- [282] Sgambitterra, E., Magaro, P., Niccoli, F., Renzo, D. and Maletta, C. “Novel insight into the strain-life fatigue properties of pseudoelastic NiTi shape memory alloys”. In: *Smart Mater. Struct.* 28 (2019), 10LT03.
- [283] Wheeler, R., Smith, J., Ley, N., Giri, A. and Young, M. “Shape Memory Behavior of Ni49.5Ti50.5 Processing-Induced Strain Glass Alloys”. In: *TMS 2019 148th Annual Meeting & Exhibition Supplemental Proceedings*. Minerals Metals & Materials Series. Springer International Publishing AG, Cham, Switzerland, 2019, pp. 1411–1420.
- [284] Young, B., Haghgouyan, B., Lagoudas, D. and Karaman, I. “Effect of Temperature on the Fracture Toughness of a NiTiHf High Temperature Shape Memory Alloy”. In: *Shap. Mem. Superelasticity* 5 (2019), pp. 362–373.
- [285] Bian, X., Saleh, A., Lynch, P., Davies, C., Pereloma, E. and Gazder, A. “An in-situ synchrotron study of the B2 → B19' phase transformation in a Ni-Ti alloy subjected to uniaxial monotonic tension”. In: *Mater. Sci. Eng. A* 743 (2019), pp. 327–338.
- [286] Sgambitterra, E., Maletta, C., Magaro, P., Renzo, D., Furgiuele, F. and Sehitoglu, H. “Effects of Temperature on Fatigue Crack Propagation in Pseudoelastic NiTi Shape Memory Alloys”. In: *Shap. Mem. Superelasticity* 5 (2019), pp. 278–291.
- [287] Sgambitterra, E., Magaro, P., Niccoli, F., Renzo, D. and Maletta, C. “Low-to-high cycle fatigue properties of a NiTi shape memory alloy”. In: *25th International Conference on Fracture and Structural Integrity*. Ed. by F. Iacoviello, L. Susmel, D. Firrao and G. Ferro. Vol. 18. Procedia Structural Integrity. Elsevier Science BV, Amsterdam, Netherlands, 2019, pp. 908–913.
- [288] Zeng, Z., Cong, B., Oliveira, J., Ke, W., Schell, N., Peng, B., Qi, Z., Ge, F., Zhang, W. and Ao, S. “Wire and arc additive manufacturing of a Ni-rich NiTi shape memory alloy: Microstructure and mechanical properties”. In: *Addit. Manuf.* 32 (2020), p. 101051.
- [289] Paranjape, H., Ng, B., Ong, I., Vien, L. and Huntley, C. “Phase transformation volume amplitude as a low-cycle fatigue indicator in nickel-titanium shape memory alloys”. In: *Scr. Mater.* 178 (2020), pp. 442–446.
- [290] Suhail, R., Chen, J., Amato, G. and McCrum, D. “Mechanical behaviour of NiTiNb shape memory alloy wires - Strain localization and effect of strain rate”. In: *Mech. Mater.* 144 (2020), p. 103346.

- [291] Mohajeri, M., Case, R., Haghgouyan, B., Lagoudas, D. and Castaneda, H. “Loading influence on the corrosion assessment during stress-induced martensite reorientation in nickel-titanium SMA”. In: *Smart Mater. Struct.* 29 (2020), p. 035013.
- [292] Zhao, H. and Andrawes, B. “Innovative prestressing technique using curved shape memory alloy reinforcement”. In: *Constr. Build. Mater.* 238 (2020), p. 117687.
- [293] Suhail, R., Amato, G. and McCrum, D. “Heat-activated prestressing of NiTiB shape memory alloy wires”. In: *Eng. Struct.* 206 (2020), p. 110128.
- [294] Sidharth, R., Wu, Y., Brenne, F., Abuzaid, W. and Sehitoglu, H. “Relationship Between Functional Fatigue and Structural Fatigue of Iron-Based Shape Memory Alloy FeMnNiAl”. In: *Shape Mem. Superelasticity* 6 (2020), pp. 256–272.
- [295] Li, C., Ao, S., Oliveira, J., Cheng, M., Zeng, Z., Cui, H. and Luo, Z. “Ultrasonic spot welded NiTi joints using an aluminum interlayer: Microstructure and mechanical behavior”. In: *J. Manuf. Process.* 56 (2020), pp. 1201–1210.
- [296] Reedlunn, B., LePage, W., Daly, S. and Shaw, J. “Axial-torsion behavior of superelastic tubes: Part I, proportional isothermal experiments”. In: *Int. J. Solids Struct.* 199 (2020), pp. 1–35.
- [297] Su, T., Lu, N., Chen, C. and Chen, C. “Full-field stress and strain measurements revealing energy dissipation characteristics in martensitic band of Cu-Al-Mn shape memory alloy”. In: *Mater. Today Commun.* 24 (2020), p. 101321.
- [298] Samothrakitis, S., Larsen, C. B., Woracek, R., Heller, L., Kopeček, J., Gerstein, G., Maier, H. J., Rameš, M., Tovar, M., Šittner, P., Schmidt, S. and Strobl, M. “A multiscale study of hot-extruded CoNiGa ferromagnetic shape-memory alloys”. In: *Mater. Des.* 196 (2020), p. 109118.
- [299] Aycock, K., Weaver, J., Paranjape, H. M., Senthilnathan, K., Bonsignore, C. and Craven, B. “Full-field microscale strain measurements of a nitinol medical device using digital image correlation”. In: *J. Mech. Behav. Biomed. Mater.* 114 (2021), p. 104221.
- [300] Shen, V., Bumgardner, C., Actis, L., Ritz, J., Park, J. and Li, X. “3D digital image correlation evaluation of arthrodesis implants”. In: *Clin. Biomech.* 71 (2020), pp. 29–36.
- [301] Suhail, R., Amato, G. and McCrum, D. “Heat-activated prestressing of NiTiNb shape memory alloy wires”. In: *Eng. Struct.* 206 (2020), p. 110128.
- [302] Xiao, R., Hou, B., Sun, Q., Zhao, H. and Li, Y. “An experimental investigation of the nucleation and the propagation of NiTi martensitic transformation front under impact loading”. In: *Int. J. Impact Eng.* 140 (2020), p. 103559.
- [303] Shariat, B. “Experimental Investigation of Heterogeneous Strain Fields Created in Metallic Materials”. In: IOP Conference Series- Materials Science and Engineering 831 (2020), p. 012006.
- [304] Safaei, K., Nematollahi, M., Bayati, P., Dabbaghi, H., Benafan, O. and Elahinia, M. “Torsional behavior and microstructure characterization of additively manufactured NiTi shape memory alloy tubes”. In: *Eng. Struct.* 226 (2021), p. 111383.
- [305] Paranjape, H., Aycock, K., Bonsignore, C., Weaver, J., Craven, B. and Duerig, T. “A probabilistic approach with built-in uncertainty quantification for the calibration of a superelastic constitutive model from full-field strain data”. In: *Comput. Mater. Sci.* 192 (2021).
- [306] Abut, B., Haghgouyan, B., Karaman, I. and Lagoudas, D. “Effect of Specimen Thickness on the Fracture Toughness of a NiTi Shape Memory Alloy”. In: *Shap. Mem. Superelasticity* 7 (2021), pp. 90–100.
- [307] Sgambitterra, E., Magaro, P., Niccoli, F., Furguele, F. and Maletta, C. “Fatigue Crack Growth in Austenitic and Martensitic NiTi: Modeling and Experiments”. In: *Shap. Mem. Superelasticity* 7 (2021), pp. 250–261.

- [308] Bauer, A., Vollmer, M. and Niendorf, T. “Effect of Crystallographic Orientation and Grain Boundaries on Martensitic Transformation and Superelastic Response of Oligocrystalline Fe-Mn-Al-Ni Shape Memory Alloys”. In: *Shap. Mem. Superelasticity* 7 (2021), pp. 373–382.
- [309] Elibol, C. “Superelastic anisotropy and meso-scale interface regions in textured NiTi sheets”. In: *J. Fac. Eng. Archit. Gazi Univ.* 36 (2021), pp. 2121–2133.
- [310] Patriarca, L., Abuzaid, W., Carlucci, G., Belevi, F. and Casati, R. “Pseudoelasticity in FeMn-NiAl shape memory alloy lattice structures produced by Laser Powder Bed Fusion”. In: *Mater. Lett.* 302 (2021), p. 130349.
- [311] Su, T., Lu, N., Chen, C. and Chen, C. “On the Decrease in Transformation Stress in a Bicrystal Cu-Al-Mn Shape-Memory Alloy during Cyclic Compressive Deformation”. In: *Materials* 14 (2021), p. 4439.
- [312] Xiao, R., Hou, B., Sun, Q., Zhao, H. and Li, Y. “Mechanical behaviors of polycrystalline NiTi SMAs of various grain sizes under impact loading”. In: *Sci. China Ser. E: Technol. Sci.* 64 (2021), pp. 1401–1411.
- [313] Qing, X., Qin, Y. and Dai, F. “Experimental investigation of micromechanical behavior of advanced materials by moiré interferometry”. In: *Opt. Lasers Eng.* 25 (1996), pp. 179–189.
- [314] Zhang, X., Sun, Q. and Yu, S. “On the Strain Jump in Shape Memory Alloys. A Crystallographic-Based Mechanics Analysis”. In: *Acta Mech. Sin.* 15 (1999), pp. 134–144.
- [315] Sun, Q., Xu, T. and Zhang, X. “On Deformation of A-M Interface in Single Crystal Shape Memory Alloys and Some Related Issues”. In: *J. Eng. Mater. Technol. ASME* 121 (1999), pp. 38–43.
- [316] Xiangyang, Z., Qingping, S. and Yu, S. “A non-invariant plane model for the interface in CuAlNi single crystal shape memory alloys”. In: *J. Mech. Phys. Solids* 48 (2000), pp. 2163–2182.
- [317] Tse, K. and Sun, Q. “Some Deformation Features of Polycrystalline Superelastic NiTi Shape Memory Alloy Thin Strips and Wires under Tension”. In: *Advances in Engineering Plasticity, PTS 1-2*. Ed. by T. Yu, Q. Sun and J. Kim. Vol. 177-1. Key Engineering Materials. Trans Tech Publications Ltd, Zurich, Switzerland, 2000, pp. 455–460.
- [318] Fang, D., Liu, J., Xu, G. and Dai, F. “Micromechanical study of formation and evolution of martensite for Cu-Al-Ni single crystal by moiré interferometry”. In: *Theor. Appl. Fract. Mech.* 33 (2000), pp. 49–55.
- [319] Jonnalagadda, K. D., Sottos, N. R., Qidwai, M. A. and Lagoudas, D. “In situ displacement measurements and numerical predictions of embedded SMA transformation”. In: *Smart Mater. Struct.* 9 (2000), pp. 701–710.
- [320] Du, H., Xie, H., Jiang, H., Rong, L., Luo, Q., Gu, C. and Zhao, Y. “Strain Analysis on Porous TiNi SMA Using SEM Moiré Method”. In: *Experimental Mechanics in Nano and Biotechnology, Pts 1 and 2*. Ed. by S. Lee and Y. Kim. Vol. 326–328. Key Engineering Materials. Trans Tech Publications Ltd, Zurich, Switzerland, 2006, pp. 79–82.
- [321] Perry, K. E., Labossiere, P. E. and Steffler, E. “Measurement of Deformation and Strain in Nitinol”. In: *Exp. Mech.* 47 (2007), pp. 373–380.
- [322] Du, H., Xie, H., Guo, Z., Pan, B., Luo, Q., Gu, C., Jiang, H. and Rong, L. “Large-deformation analysis in microscopic area using micro-moiré methods with a focused ion beam milling grating”. In: *Opt. Lasers Eng.* 45 (2007), pp. 1157–1169.
- [323] Xie, H., Kishimoto, S., Li, Y., Liu, D., Zhang, M. and Hu, Z. “Deformation Analysis of Shape Memory Alloy Using SEM Scanning Moiré Method”. In: *Advances in Fracture and Materials Behavior, PTS 1-2*. Ed. by W. Yang, M. Geni, T. Wang and Z. Zhuang. Vol. 33–37. Advanced Materials Research. Trans Tech Publications Ltd, Zurich, Switzerland, 2008, p. 675.

- [324] Wang, Q., Xie, H., Jiang, H., Li, Y., Dai, F., Chen, P., Zhang, Q. and Huang, F. “Investigation on the Deformation of TiNi Shape Memory Alloy with a Crack Using Moiré Interferometry”. In: *Adv. Mater. Res.* 33–37 (2008), pp. 1–6.
- [325] Guo, Z., Xie, H., Dai, F., Qiang, H., Rong, L., Chen, P. and Huang, F. “Compressive behavior of 64% porosity NiTi alloy: An experimental study”. In: *Mater. Sci. Eng. A* 515 (2009), pp. 117–130.
- [326] Balandraud, X., Barrera, N., Biscari, P., Grédiac, M. and Zanzotto, G. “Strain intermittency in shape-memory alloys”. In: *Phys. Rev. B* 91 (2015), p. 174111.
- [327] Blaysat, B., Balandraud, X., Grédiac, M., Vives, E., Barrera, N. and Zanzotto, G. “Concurrent tracking of strain and noise bursts at ferroelastic phase fronts”. In: *Commun. Mater.* 1 (2020), p. 3.
- [328] Lanba, A. and Hamilton, R. “NiTi-based SMAs for Self-Post-Tensioned Bridge Girders”. In: *Proceedings of the American Society for Composites*. Ed. by C. Bakis. Vol. 2. Destech Publications, Lancaster, PA, USA, 2013, pp. 1640–1649.
- [329] Zhang, X., Feng, P., He, Y., Yu, T. and Sun, Q. “Experimental study on rate dependence of macroscopic domain and stress hysteresis in NiTi shape memory alloy strips”. In: *Int. J. Mech. Sci.* 52 (2010), pp. 1660–1670.
- [330] Pataky, G. J., Ertekin, E. and Sehitoglu, H. “Elastocaloric cooling potential of NiTi, Ni₂FeGa, and CoNiAl”. In: *Acta Mater.* 96 (2015), pp. 420–427.